Automated Segmentation of Soft tissue in Abdominal CT scans

Dennis Sher Ee Lim (B.Comp(Hons), NUS)

A THESIS SUBMITTED FOR THE DEGREE OF

MASTERS OF SCIENCE (COMPUTING)

SCHOOL OF COMPUTING

NATIONAL UNIVERSITY OF SINGAPORE

2009

July 8, 2009

Acknowledgements

I would like to thank my supervisor, Dr Leow Wee Kheng, for all the support and guidance he has given me all these years, as well as for showing me the wonderful world of computer vision. I would also like to thank him for his patience with me for all the times that I have had to delay the completion of this thesis.

I would also like to thank my esteemed colleagues from the Computer Vision Lab: Ding Feng, Lu Haiyun, Qi Yingyi, Li Hao, Song Zhiyuan, Piyush Kanti Bhunre, who have helped give advice and support, as well as performing the painstaking task of manually segmenting each CT slice to obtain the ground truth. I would also like to thank Chen Ying, a respected senior who really helped me a lot during my undergraduate and early graduate days. Next I would like to thank the radiology dept of the National University Hospital for all the data to work on.

Last but not least, I would like to thank my girlfriend, Kirsten Ee, for all her support these years, and for always bringing a smile to my face.

Dennis Lim
25 March 2009

Contents

Abstract

Patient-specific 3D models are necessary for many medical procedures. However, current techniques require manual segmentation of organs from CT or MRI images. Such a method is tedious, resulting in segmentation being done only on selected slices. Estimation of 3D volumes from this data will result in coarse models. This will affect the accuracy of any treatment or diagnosis that uses such models. A current challenge would be to develop automated or semi-automated segmentation techniques to replace this manual segmentation.

The main types of algorithm used in medical image segmentation are atlas-based algorithms. This is because medical images are often very complex and noisy. The information provided by the atlases increase the robustness of the algorithm. This produces more accurate results. This thesis proposes an automated, non probabilistic segmentation algorithm for the segmentation of the liver and other organs from abdominal CT slices. The algorithm is designed as a multi-stage pipeline. After pre-processing of the CT image, the algorithm registers the contours obtained from the atlas to the image via a global registration stage and two local registration stages. This thesis also introduces a hybrid active contour known as the Iterative Corresponding Snake. This is a combination of active contours and the Iterative Corresponding Points algorithm proposed by [Ding et al., 2005]. It exhibits greater robustness than the original active contour and is also more successful in converging to the correct edges in the target image.

The algorithm was tested for convergence, accuracy and robustness with good results. The final step would be to further enhance the robustness of the algorithm as well as extend it to three dimensions in order to produce smoother and more accurate segmentation results.

List of Figures

vii

Chapter 1

Introduction

In modern day hospitals, there is an increase in the use of computers and software solutions to aid doctors in the analysis, diagnosis and treatment of various ailments and conditions. Often, this aid comes in the form of digital imagery of various body parts (Figure 1.1[1]). Modalities include digital x-rays, CT images and MRI images. Using these images, doctors can look inside the human body without having to operate on it.

These new imaging techniques are big improvements over the more conventional, non-digital techniques used in the past. For example, digital x-rays can achieve image quality that is comparable to analog methods, but are far less noisy and can be easily analyzed by computers since they are in digital format. Furthermore, CT and MRI images provide extremely detailed cross-sectional views of the human body, something which past methods are incapable of. These mean that doctors can now obtain more accurate and precise information about the nature of the ailments that the patients are suffering from.

1.1 Background

Uses of digital imagery come in many forms. First of all, they are used for diagnosis of ailments by letting doctors see the actual problem on top of just basing diagnosis on symptoms and other non-visual information. They are also used during treatment, especially in cases

---

[1]Image from http://www.medical.siemens.com

Figure 1.1: A man getting ready for a CT scan.

where surgical procedures are required. This use of computers for surgical treatment is generally known as computer-assisted surgery. Fluoroscopic imagery (Figure 1.2[2]) gives doctors a view of the inside of the human body without cutting open the entire area, resulting in less invasive procedures, thereby hastening the recovery process. Virtual navigation systems make use of digital images and three dimensional models reconstructed from such images to determine the position and orientation of tools and human body parts, allowing doctors to perform their tasks with a great amount of precision. However, probably the most extensive use of digital imagery is during the pre-operation planning phase of the treatment. Images are used in this phase for analysis of the seriousness of the problem by providing quantitative information such as the location and size of the anomaly and its stage of development. Reconstructed three dimensional models provide excellent visualization of the target area and give doctors a better sense of the situation at hand. In conclusion, computer assisted techniques make medical procedures more accurate and precise, reducing patient risk and improving the time taken for treatment and recovery.

1.2   Motivation

The key technique required to render computer assisted techniques usable is segmentation. The computer has to know where the region of interest is before it can perform any measurements and provide any information. Needless to say the quality of the segmentation also affects the accuracy of the information returned.

An example of the use of segmentation in medical procedures is the treatment of liver ailments. One such ailment is liver failure, which requires a liver transplant for the patient. In liver transplants, doctors have to determine the best way to cut the donor's organ so as to avoid cutting the major blood vessels (Figure 1.3[3]). This is very important because cutting these by mistake may result in severe loss of blood for the patient, possibly leading to death. Moreover, doctors have to compute the volume of the different lobes of the liver in order to determine the optimal amount to cut from the donor. Cutting too much is no good as it

---

[2]Image from http://www.overlakeimaging.com/Spine.asp
[3]Image from http://www.surgery.usc.edu/divisions/hep/livedonorlivertransplant.html

3
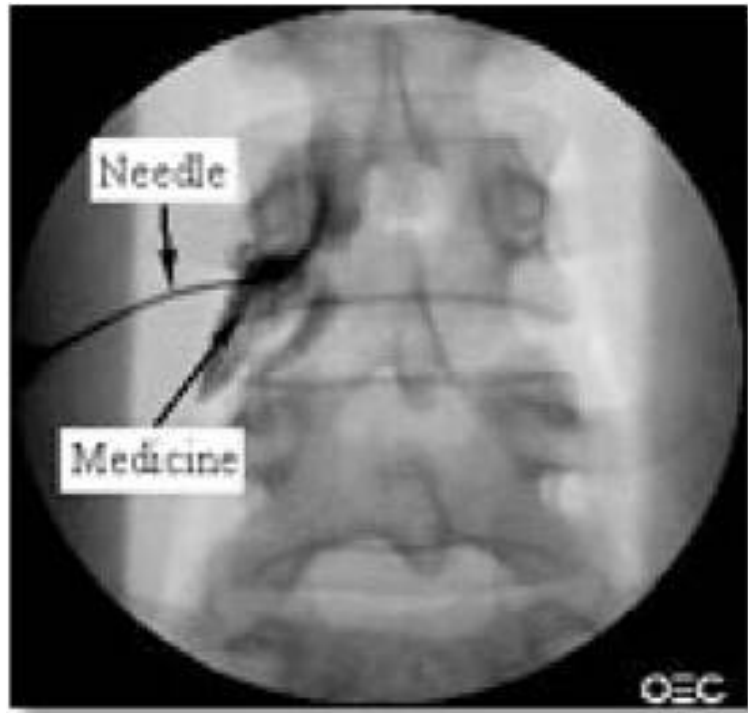
Figure 1.2: Example of fluoroscopic imagery of spine.

unnecessarily deprives the donor of a portion of his organ, thus affecting his health. Cutting too little on the other hand may have serious consequences for the recipient of the organ, who may have too little liver to function normally. Three dimensional imagery of the liver can give doctors a more accurate picture of the layout of the blood vessels in and around it, allowing doctors to pre-determine the regions to cut.

In order to create these three-dimensional models, segmentation of the organs from CT images is required. Unfortunately, software systems for automatic segmentation and quantification are not available commercially. In hospitals, doctors either perform the segmentation of CT and MRI image slices manually or pay a specialized software company to do the segmentation. Performing the segmentation in-house is very tedious, considering that a set of CT or MRI images often contain more than a hundred images. Thus, in-house manual segmentation is often performed only on a selected number of image slices, and a crude volume is estimated from there. On the other hand, outsourcing the segmentation and model building will produce a three dimensional model of better quality, but generally
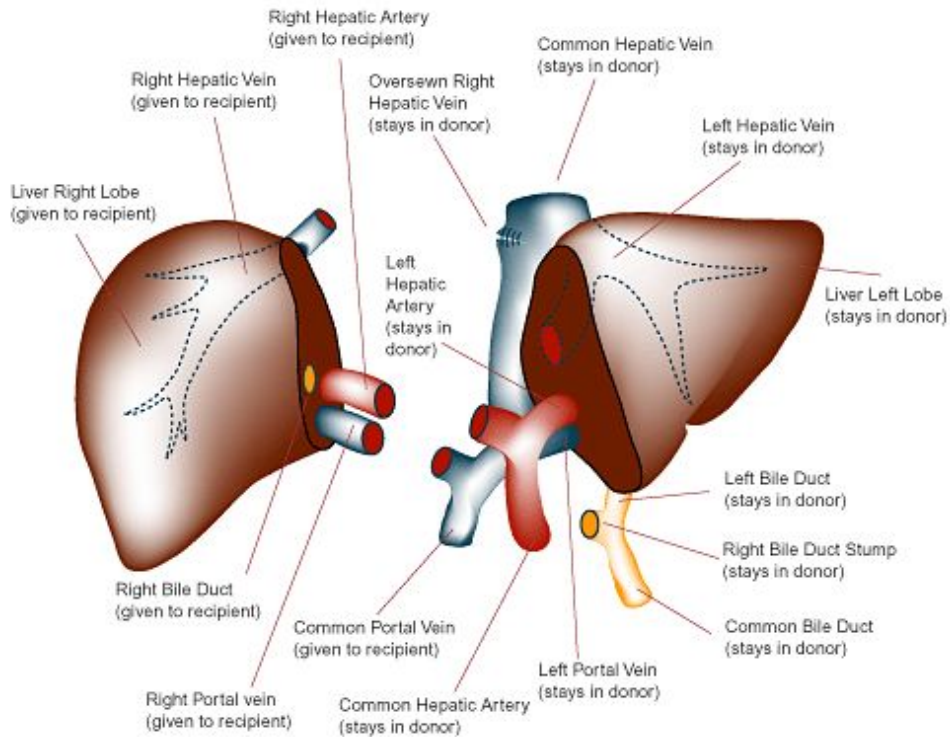
Figure 1.3: Diagram showing how a donor's liver is cut for transplant.

costs a sizeable amount of money and the results are only available after several days. For time-critical procedures like liver transplant, where the patients' lives are at stake, this waiting time could only be harmful for the patient. Interviews with surgeons in the National University Hospital (NUH) reveal that for the case of liver transplants, the error in volume estimation may go as high as 20%. Such a large error means that there is a high chance that the amount of liver cut from the donor will vary from the optimum amount by a wide margin.

Therefore, a current challenge would be to develop a system to aid doctors in performing in-house segmentation, quantification and visualization of organs in CT images. These would not only ease the workload of doctors, but also reduce the cost and time taken for the treatment of patients.

1.3   Segmentation Techniques

There are many techniques which can be used to segment medical images, and these can be generalized into two broad categories: atlas-based and non-atlas based methods. Non atlas-based methods basically make use of only the information that can be directly obtained from the image to perform segmentation. This information included edges, intensity and texture. While such methods are easy to implement and have relatively faster run-times as compared to atlas-based methods, they are less accurate since they do not make use of any information of the shape and location of the target region. This means that the risk of having the algorithm trapped in a local minimum is very high. This does not mean that the quality of segmentation of non atlas-based methods will be low, but to guarantee high precision segmentation by just using non atlas-based approaches, a lot of human intervention is needed.

Atlas-based methods incorporate information about shape and location of the desired organs into the segmentation algorithm. This requires the use of an atlas or model to store the information. This improves the accuracy of the algorithm as the domain knowledge provided by the atlas improves the robustness of the algorithm, enabling it to avoid more false positives. Also, the use of atlases for segmentation allow for the creation of fully automatic algorithms since the atlases can be used to initialize the segmentation. This makes atlas-based methods more desirable for medical image segmentation, where the segmentation problem is non-trivial and the chance of human error is high.

There are two types of atlas-based segmentation. The first type makes use of statistical or probabilistic models to find the best fitting match (Figure 1.4[4]). These models typically store statistical distributions of information obtained from a set of training images, such as pixel intensity, object shape, size and location. The advantage of a statistical model is that you can definitely converge to the correct solution given infinite time and a training set with infinite samples. However, that is also the main disadvantage of a probabilistic approach to segmentation. It is impossible to have an infinite training set, so an approximation of a large training set size is needed. However, it cannot be determined if a training set is large enough for the work it needs to perform, nor can there be any guarantees that the train-

---

[4]Image from http://www.zib.de/visual/projects/liverSurgery/liverSurgerylong.en.html
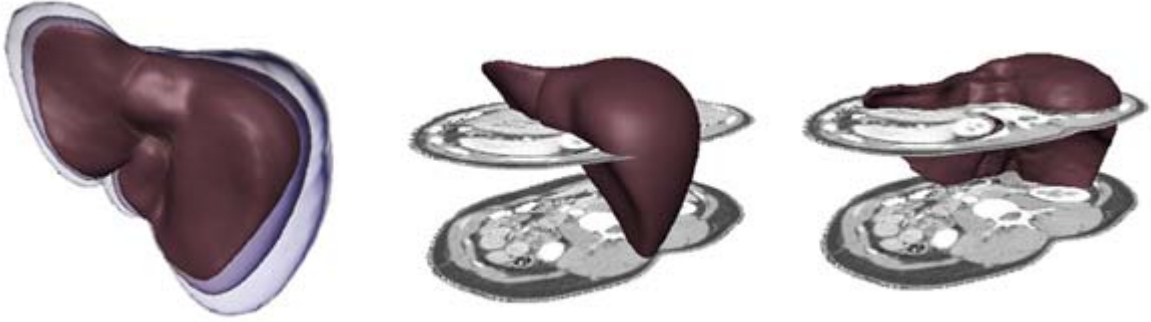
Figure 1.4: Illustration of using a statistical model for model-based segmentation. On the left is the model showing three different statistical shape variations. The algorithm is initialized as per the middle diagram and the final result is on the right.

ing set will encompass the correct solution., in which case the algorithm will undoubtedly fail.

The second type of atlas-based segmentation is the non-probabilistic approach, where only a single object is used as the atlas. This object is typically a set of features retrieved from a single image, but can also include other external information as well. The main advantage of a non-probabilistic approach over a probabilistic one is that there is no need for a large training set, so it can be use even in situations where training data is scarce. Also, a non-probabilistic approach is likely to be more robust when faced with a target that differs greatly from the model, as it is not constrained to a certain range as with probabilistic models. However, it is more prone to be trapped in local minima, so clever choices must be made for the features used for segmentation.

More examples of the different approaches for segmentation will be given later in the related works section.

1.4 Objective

The main objective of this thesis is to implement an automated atlas-based segmentation algorithm for segmenting multiple organs from abdominal CT images. A non-probabilistic

approach is used due to the lack of large numbers of abdominal CT data sets. A secondary objective is to make the algorithm robust so that it can handle significant variations in the shape and location of the targets of interest. This is done by applying the same atlas across different images within the same data set, as well as testing the atlas with different data sets.

This thesis proposes a segmentation framework capable of segmenting different body parts by simply replacing the atlas. The abdominal region of the body is used in this thesis due to availability of data and the challenge posed by the complicated nature of the anatomy. This framework is robust and the results obtained are accurate.

1.5   Outline of paper

In Chapter 2, a review of the existing work done in the area of medical image segmentation is performed. The focus is on the two main atlas based approaches as well as the underlying techniques used to achieve the desired results. In Chapter 3, an analysis of characteristics of human body tissue and CT images used as input to the algorithm is carried out. This is to determine how these characteristics add to the complexity of the problem. In Chapter 4, the techniques and methods used in the proposed algorithm are discussed in detail. Chapter 5 will describe the test setups and results. Finally, Chapter 6 will summarize on what has been achieved and discuss any further research that can be done in this area.

Chapter 2

Related Works

The main focus of this thesis is a segmentation algorithm. As such, an in-depth study into the techniques for segmentation available will help in the understanding of the problem. First, the various basic segmentation methods usually incorporated into the atlas-based algorithms are explored. This will be followed by a review on the two main types of atlas-based segmentation: probabilistic and non-probabilistic atlas-based segmentation. This is because atlas-based algorithms are the most common form of segmentation algorithm used in medical image segmentation. Finally, as the liver is the focus of this thesis, a review of various work done on liver segmentation is done.

2.1 Common Techniques used in Medical Image Segmentation

While the emphasis in this thesis are atlas-based segmentation algorithms, it is nevertheless important to review the underlying techniques which atlas-based algorithms are based upon. Some of the more common ones are:

- Thresholding

- Edge-based Segmentation

- Region-based Segmentation

- Watershed Transform

- Active Contours

- Level Sets

Each of these techniques will be looked at in turn.

2.1.1 Thresholding

Thresholding or histogram clustering is a general technique for segmentation that relies on intensity values to differentiate between separate regions [1]. This is illustrated for two dimensions by the following equation:

$$y = \begin{cases} 1 & \text{if } I_{ij} < \epsilon \\ 0 & \text{otherwise} \end{cases}$$

Where I_{ij} is a point in a two-dimensional image and ϵ is the threshold level.

The key is to find the optimum value to separate the regions into. The usual approach to doing so is to plot a histogram of the intensities of the pixels in the image. The optimum threshold value would then be the point that separates the two main peaks within the histogram. This is shown in Figure 2.1.

Thresholding is extremely easy to implement and works well for images that are unimodal, meaning there is only one main peak in the intensity histogram. However, most natural images have multimodal intensities. This severely reduces the ability of thresholding algorithms to effectively segment the images. Histogram clustering improves on standard thresholding by clustering pixels into multiple bins, hence improving performance for multimodal images.

Despite the limited scope in which thresholding segmentation can be applied, people nonetheless have tried to modify the original algorithm to handle multimodal images. For

---

[1]http://www.ph.tn.tudelft.nl/Courses/FIP/noframes/fip.html
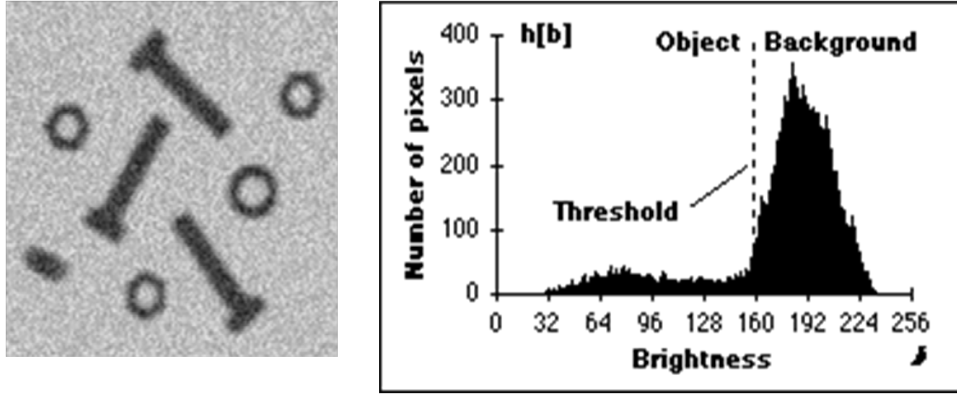
Figure 2.1: Illustration and intensity histogram with dotted line showing the optimal place to put the threshold

example, [Tobias and Seara, 2002] proposed a thresholding segmentation algorithm which determines the optimum value to threshold via the use of fuzzy sets. [Arifin and Asano, 2006] also introduces a similarity measure based on inter-class and intra-class variance to set good threshold measures for segmentation. Mutual Information (MI) is another measure that can be used to determine the clustering of the histogram bins. [Rigau et al., 2004] proposes a two step algorithm in which the image is first segmented into homogeneous regions by maximising the MI gain of the channel from the histogram bins to the regions of the partitioned image, and then followed by the clustering of the intensity bins via the minimizing the information loss of the reversed channel.

While thresholding techniques are usually simple to implement and can run rather quickly, they have the disadvantage that it may be difficult to identify significant peaks in the image. This is particularly true in the case of medical images like MR and CT, where multiple objects can have similar intensities.

2.1.2   Edge-based Segmentation

Edge-based techniques look for the contour along which there is a change in the differentiating feature along the normal of the contour. This contour is known as the edge. Common
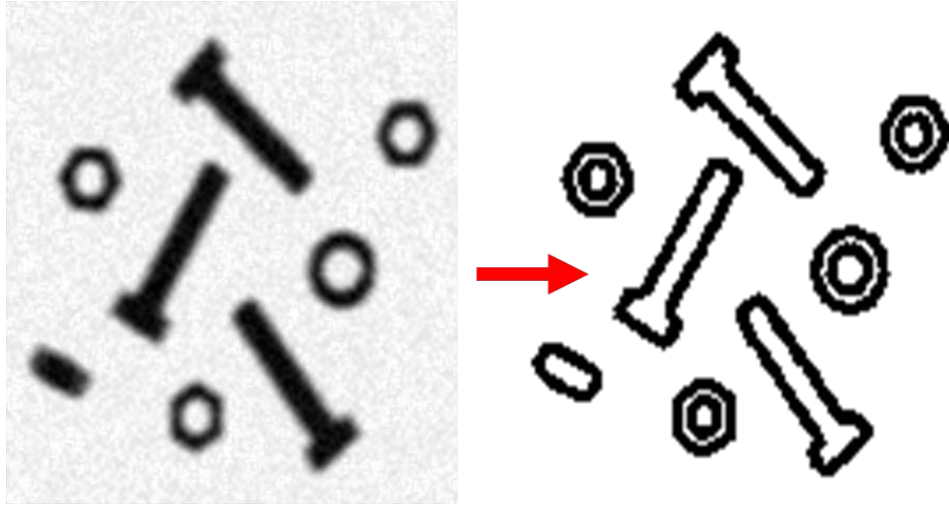
Figure 2.2: Illustration of the segmentation of objects in an image via an edge-based segmentation algorithm

features that are used include intensity, colour and texture. An example using intensity as the differentiating feature is shown below in Figure 2.2.

[Brejl and Sonka, 1998] incorporated machine learning into an edge-based segmentation method to segment medical ultrasound images. The results they obtained through their program are comparable to manual segmentation done by experts. [Godbole and Amin, 1995] proposed the use of mathematical morphology to perform edge and overlap detection in lung images taken with a gamma ray camera. This main advantages of using mathematical morphology are its flexibility and the ability to implement it in hardware to achieve real time speeds.[Liu et al., 2007b] also proposed the use of morphological operations to implement a robust edge detector for the detection of edges in ultrasound heart ventricular wall images.

Edge-based segmentation is very popular for use as a pre-processing step in the more sophisticated segmentation algorithms like active contours, level sets and atlas-based segmentation. Active contours and level sets will be discussed in Sections .

Edge-based segmentation techniques are good in many cases where the images are relatively noise free and there is high contrast between objects in the images. However, medical
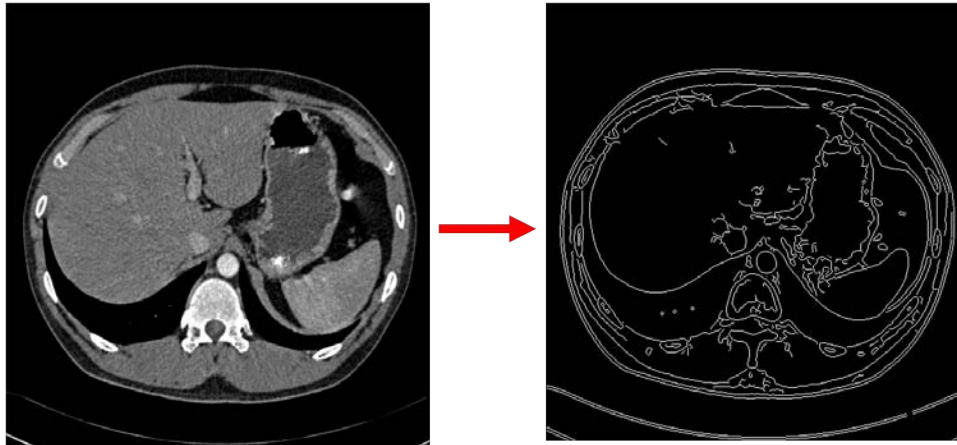
Figure 2.3: Sample CT image (left) and its corresponding edge map (right). Observe the many gaps in the contours as well the cluttered edges in some areas. These will confuse segmentation algorithms.

images tend to be cluttered and noisy. Also, they often have poor contrast between two organs. These result in broken edges and noise in the edge images (Figure 2.3). This makes generic edge-based techniques less viable for medical segmentation. Even edge-based techniques which segment based on changes in texture will not work well because of the uniformity of the texture of soft tissue, as discussed in Sections 2.1.5 and 2.1.6

2.1.3 Region-based Segmentation

Region based segmentation techniques perform segmentation by grouping pixels or areas based on some uniformity criterion of the region's characteristics. This uniformity criterion is usually based on intensity, colour, texture or a combination of them. This approach to segmentation assumes that adjacent regions have different characteristics.

There are basically two types of region based approaches. The first is the region merging approach. What this does is to place seeds throughout the input image. Next, the region near to these seeds is checked to see if they satisfy the uniformity criterion. If they do, they are added to the seed region. This is done iteratively, resulting in regions that grow until no more neighbouring areas matching the criterion can be found. If two regions with the
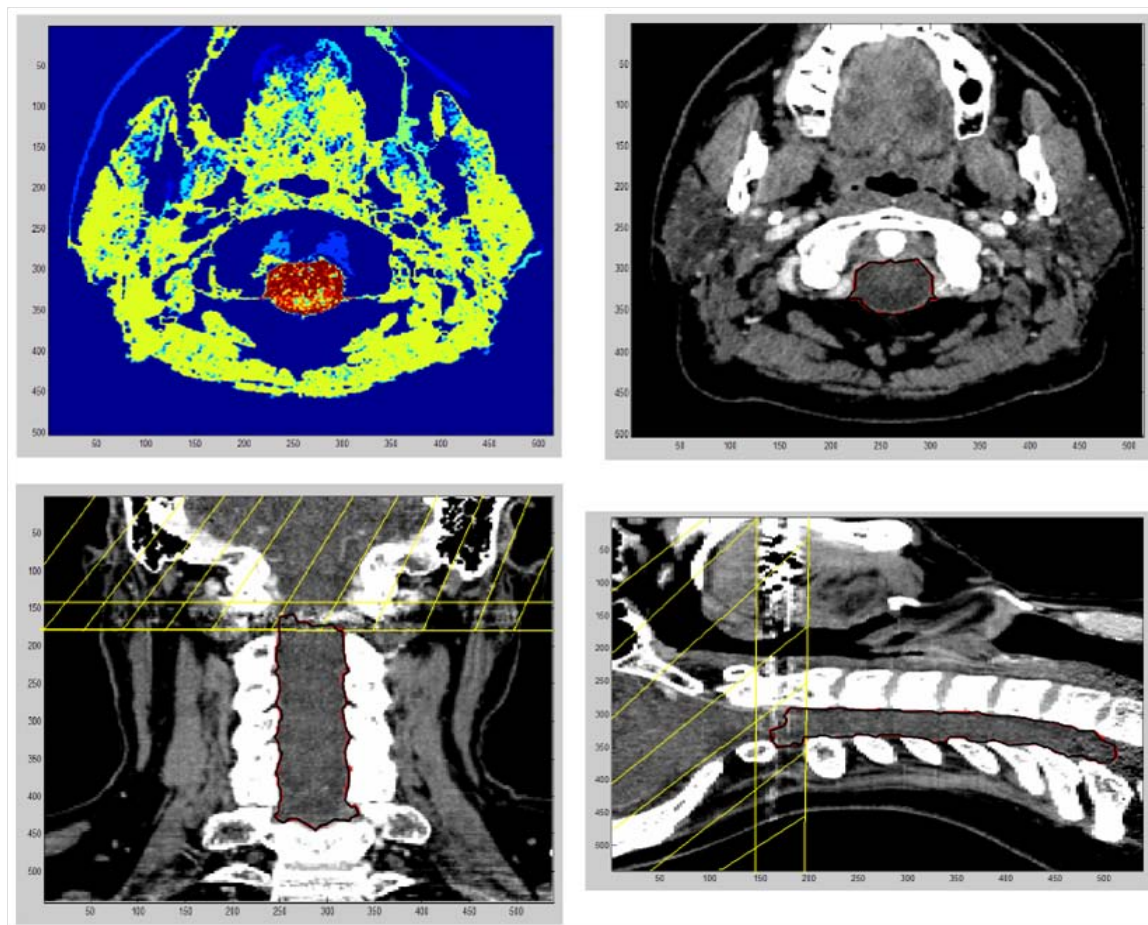
Figure 2.4: Segmentation of the spine via region-growing. The image on the top-left shows how the different parts of the body are clustered. The other three images show the segmentation of the spine from three different angles.

same criterion meet, they will merge into a single region. One example of work using this approach was proposed by [Mancas et al., 2005], who used a region growing technique to segment objects in medical images, with the uniformity criterion being intensity. The authors incorporated the spatial distance of a point to the seed into the region-growing algorithm, resulting in a map which clusters pixels based on their intensity similarity to that of the seed as well as how far the pixel is from the seed. The results of the experiments by the author show that their region-growing method can accurately segment objects from noisy medical images. An example showing spinal cord segmentation is given in Figure 2.4.

Another example of an approach that uses region growing for medical image segmentation is proposed by [Pohle and Toennies, 2001], who developed an algorithm that learns its homogeneity criterion from the characteristics of the target region. This reduces the probability of poor performance due to the selection of an unsatisfactory seed location.

The other approach is known as region splitting. The input image is defined as a single region, which is then iteratively split into smaller regions until no more splits are possible. The resultant will be the segmented image. An improvement to the standard region splitting approach is known as "split and merge". The additional feature of this approach is that sometime in regular region spitting algorithms, over-segmentation may occur where two neighboring regions that have the same region characteristics is split. The improved approach will try to merge these over-segmented regions. [Liu and Sclaroff, 2004] used a merge and split algorithm to perform segmentation. His approach is also model-guided, which is something that we will discuss in a later sub-section.

Region based techniques generally perform well for images where the regions in the image satisfy the uniformity criterion and obeys the assumption. However in practice this is seldom the case because natural images are usually noisy and the borders between objects are not always clearly defined. Furthermore, region based approaches are highly dependent on factors like the size of the seeds and the parameters of the uniformity criterion. A bad placement of the seeds may leave some regions unsegmented, while choosing inappropriate parameters for the uniformity criterion may result in separate regions which do not belong together being grouped together or a single region being split by mistake.
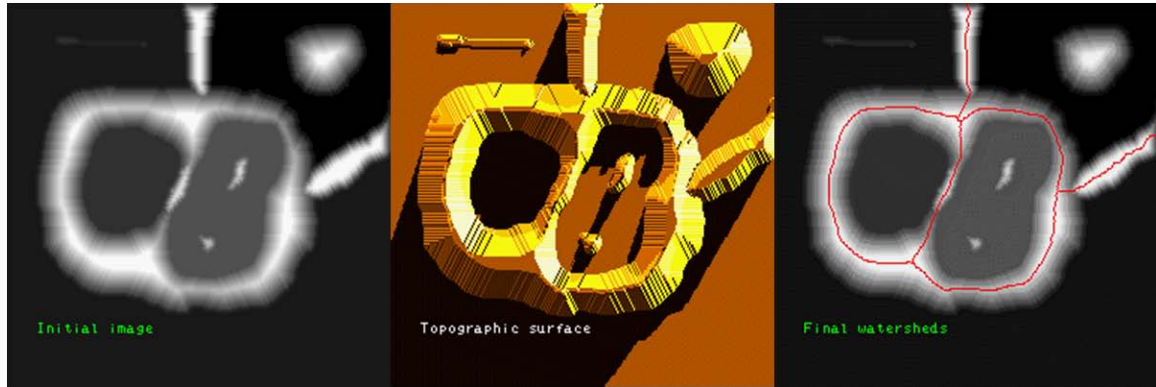
Figure 2.5: The left most image shows the initial image. The centre image is the topographical representation of the image, and the final image is the result with the red lines depicting the segmented regions.

2.1.4 Watershed Transform

The watershed transform is a type of image segmentation algorithm which was derived from the natural phenomenon of watersheds and catchment basins. Watershed transforms are similar to region-based algorithms in that they split an image into areas. This splitting is done based on the topology of the image, with the gray level of the image used to represent the height of a point. Flooding is then performed iteratively from marker points until watersheds with adjacent catchment basins are constructed. Figure 2.5[2] gives a graphical illustration of how a watershed algorithm works.

The watershed transform has the useful properties of being simple and intuitive, and it can be parallelized, making it attractive for use in real-time applications. However, it is sensitive to noise, and it is prone to over-segmentation in complicated images, such as medical images.

[Chen and Liu, 2005] is an example of the watershed transform being applied to medical image segmentation. [Grau et al., 2004] and [Straka et al., 2003a] improve on the basic implementation of the watershed transform by the addition of prior information from an

---

[2]Images courtesy of http://cmm.ensmp.fr/ beucher/wtshed.html

atlas to reduce the amount of over-segmentation. Also, [Haris et al., 1998] proposed a hybrid approach of using the watershed transform and region-merging to overcome the over-segmentation issue.

2.1.5 Active Contours

Another common segmentation method used in medical segmentation is the active contour model. This method was originally proposed by [Kass et al., 1987] in 1987, and was originally designed to perform contour extraction. Since then it has been used by many for medical image segmentation.

The active contour model works by iteratively deforming an arbitrary contour until it reaches the desired boundary, which is our object of interest in the image. It is formulated as an energy-minimizing contour controlled by two types of energies:

1. Internal energy, E_{int}, which enforces smoothness constraint.

2. External energy, E_{ext}, which guides the contour towards the configuration with the least energy

E_{int} is formulated as Equation 2.1. $\alpha(s)$ controls the malleability of the contour by restricting the allowed separation between neighbouring points. $\beta(s)$ controls the flexibility of the contour.

$$E_{int} = \frac{1}{2}(\alpha(s)|v'(s)|^2 + \beta(s)|v''(s)|^2) \tag{2.1}$$

E_{ext} is composed of the image forces that attract the snake. Generally, these are the edges in the input images. The image forces, E_{image}, are represented by gradient vectors around the edges which guide nearby contours towards the edges. These are illustrated in Figure 2.6 as the arrows pointing towards the edges.

Therefore, the total energy of the snake, E_{snake} is the integral of the sum of the internal energy, E_{int}, and the external energy, which is represented by the image energy, E_{image}
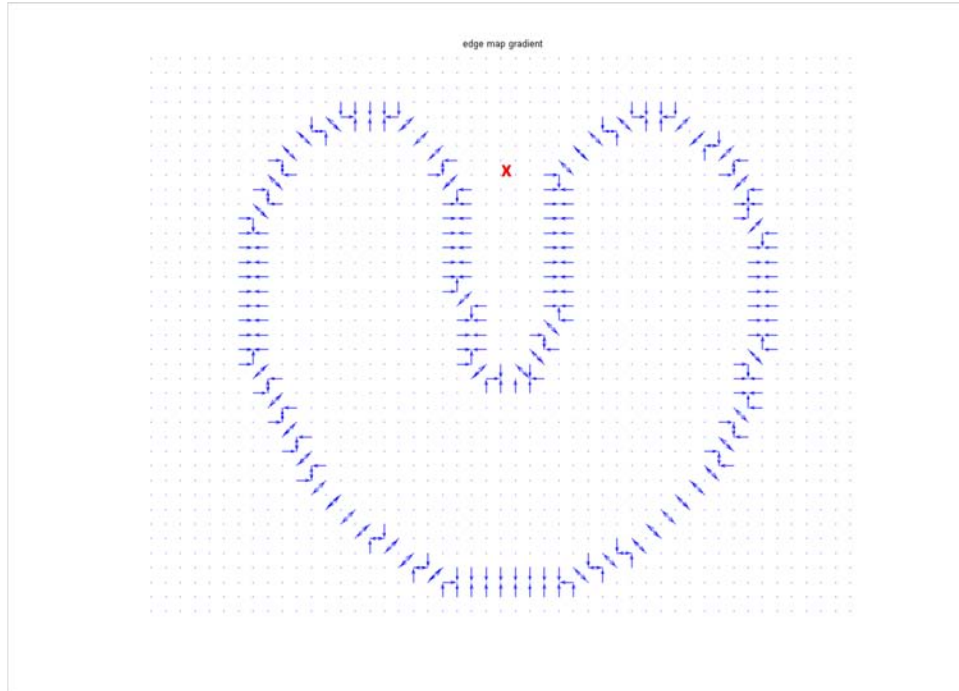
Figure 2.6: Illustration of the gradient vectors around the edges of an object

$$E_{snake} = \int_0^1 E_{int}(v(s)) + E_{image}(v(s)) \; ds \qquad (2.2)$$

The snake is iterated until E_{snake} is minimized. This configuration of minimum energy represents the final configuration of the snake.

The advantages of using a snake is that E_{int} is a built-in regularization function for the contour. This maintains the smoothness of the contour without an additional regularization step. Also, it is easy to add prior information into the active contour by modifying E_{int} or E_{image}. This was demonstrated in [Chen et al., 2005] which added curvature constraints to the active contour to control the shape of the contour. This improves the robustness of the algorithm especially in the case of noisy images. Furthermore, the forces that guide the contour can be derived from any form of correspondence simply by replacing the direction vectors representing the image energy in E_{image} with direction vectors obtained via the correspondence function. This ease of incorporating prior information and the regularization capability of active contours are the main reasons that active contours are extensively used

in this proposal.

However, the snake can be easily trapped in local minima. This is because it only utilizes edge information to perform its deformation. Since it is impossible for the algorithm to differentiate between edges of different body parts, there is no way to guarantee that the registration is correct. Another problem is that this version of snake cannot handle concave edges well. This is because there are no forces in the empty space which will pull the snake into the concave area. Therefore, the contour is largely influenced by its internal forces and adopts the minimal energy position defined by the internal forces, which is a straight line. In Figure 2.6, a point at the position marked by the red "X" would not move towards any edge as there are no forces at its position to guide it. The Gradient Vector Flow method, or GVF, is designed to mitigate this.

Gradient Vector Flow (GVF)

GVF [Xu and Prince, 1998] was created to overcome the problem of poor convergence to concave edges. It does so by diffusing the gradient vectors into the surrounding space. This results in contours being guided to the edges even if they were initialized far away. Figure 2.7 shows the difference between the gradient vector field and gvf field of the same edge map. Note that in the gvf field, the forces are present throughout the spatial domain of the image, unlike the gradient vector field where the forces are concentrated solely at the edge locations.

GVF replaces the gradient vector field as the image force in Equation 2.2. The poor convergence to concave edges is addressed by GVF because the GVF forces pull the contour into the concave areas. This is shown in Figure 2.8 in where the contour, represented by the red lines is pulled into the concave area of the object.

The addition of GVF to the original active contour resulted in significant improvements to the active contours ability to extract regions. This makes it more feasible to use active contours for medical image segmentation, as a lot of concave edges are usually present in these images.
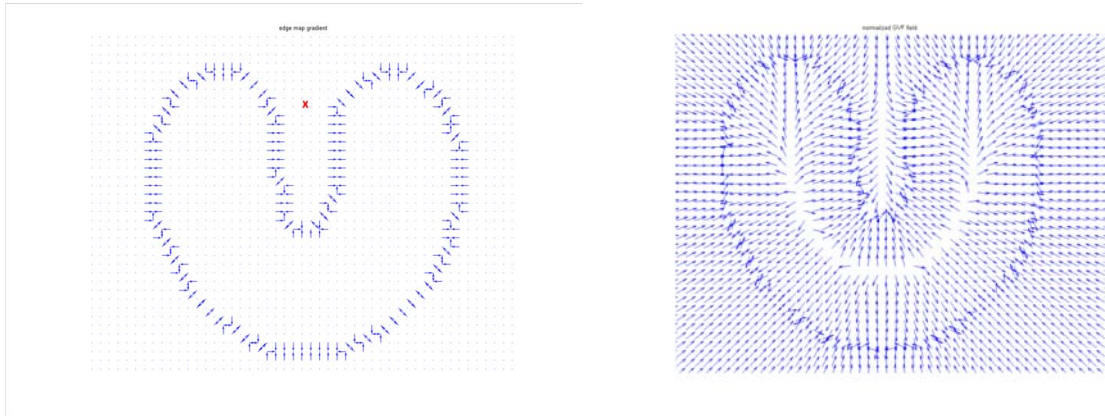
Figure 2.7: Comparison of the gradient vector field and the gvf field of an image
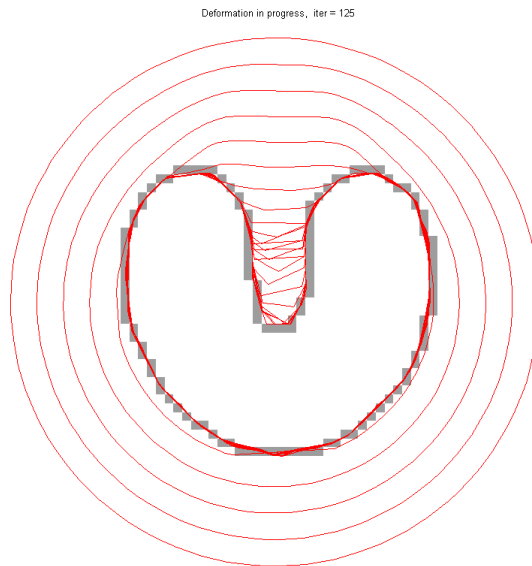
Figure 2.8: Diagram showing the red contour being guided into a concave area by GVF

Applications of active contours

A few examples of the applications and variants of active contours are briefly discussed here. As mentioned above, [Chen et al., 2005] proposed adding a curvature constraint to active contours through the use of an atlas to limit the amount of shape variation the contour is allow to have. This was applied to femur x-rays with good results. [Atkins and Mackiewich, 1996] used active contours to detect the intracranial boundary, using a mask that was created via anisotropic diffusion and thresholding as a seed. Another method proposed by [Boscolo et al., 2002] used a priori knowledge of the anatomical structure in question to guide the evolution of the active contour . This statistical information is then incorporated into the energy function of the active contour to constrain the ways that it can deform. This active contour was then applied to several different types of medical images. [Liu et al., 2007a], [Chen et al., 2008], [Slabaugh et al., 2006] and [Cremers et al., 2001] also propose segmentation algorithms based on active contours which makes use of statistical information to guide the contour. These improve the performance of the segmentation by providing higher order information about the objects of interest, making the algorithm more robust to noise and variation.

Another study by [Ballerini and Bocchi, 2003] made used of multiple active contours that were bounded together to segment the finger bones in a human hand. These active contours made use of a genetic algorithm to determine the final contour. The strength of this approach is that the problem of being trapped in local minima is avoided by the use of the genetic algorithm. Other work incorporating the use of multiple active contours to improve segmentation include [Abe and Matsuzawa, 2000], [Kim and Hong, 2008], [Silveira and Marques, 2006] and [Elmoataz and Bloyet, 2000]

Active contours can also be easily extended to three dimensions. These three-dimensional active contours, otherwise known as active surfaces, can improve the quality of segmentation of three-dimensional objects as their regularization forces act in all directions. This is unlike the conventional active contours where the regularization forces usually only work in slices.

[Sandor and Leahy, 1997], [Zhang and Braun, 1997], [Mille et al., 2007], [Yushkevich et al., 2006] and [Yezzi and Tannenbaum, 2002] proposed using three-dimensional active contour implementations to segment various anatomical structures.

2.1.6   Level Sets

Level sets are another commonly used approach in medical image segmentation. A level set segmentation approach can be visualized as an expanding contour which can change topology. One way to think of it is a circle placed on the image. This circle expands in a constant rate and can be stopped by edges in the image. It can branch off in separate directions and when two edges meet, they will merge into one and proceed. This ability to split and merge allows level set methods to segment objects with high genus. An example of this is shown below in Figure 2.9.

The level set is implemented as follows: At any time t, we have a closed curve Γ. A distance function d is defined such that for any point (x, y) on the image plane,

1. d is positive if (x, y) is outside Γ.

2. d is zero if (x, y) is on Γ.

3. d is negative if (x, y) is inside Γ.

Over all time, the set of curves will form a surface, R. This surface is known as the level set function. By moving the image plane up and down with respect to this surface, the resultant shape-changing curve that is the intersection of the image plane and R will be the contour that was described above.

Level set methods, being able to change topology, are very effective for segmentation of soft tissue since it can handle any of the cavities, splitting or merging normally found in such tissue. Examples of such objects are veins, arteries and brains. However, they require that the edges of the objects be unbroken. Due to the nature of level set techniques, the contour will just leak out of the gaps, resulting in an incorrect segmentation of the desired object. This is unlike active contours which will be restrained by its internal forces. Furthermore,
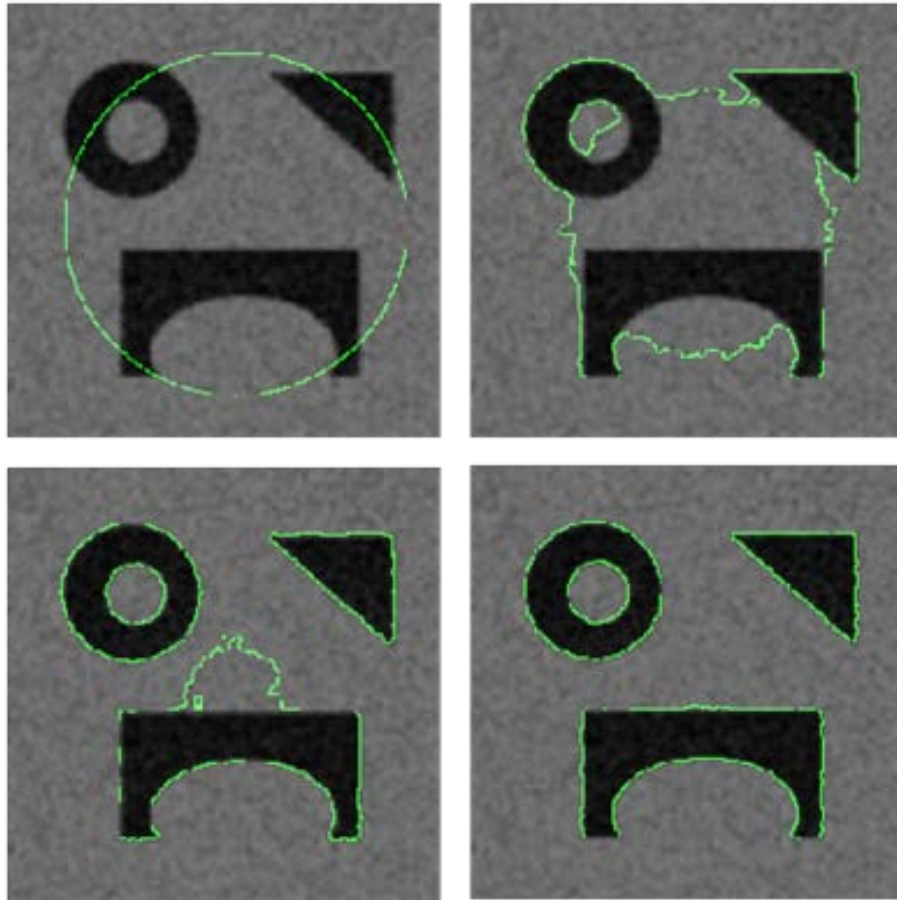
Figure 2.9: Segmentation by a level set algorithm
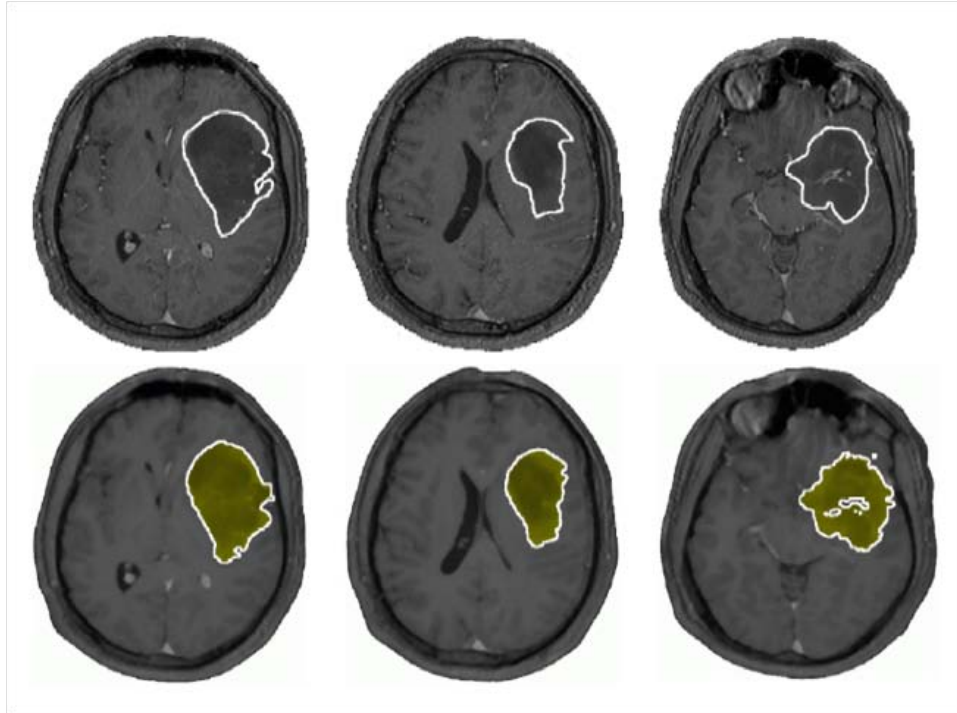
Figure 2.10: Level set segmentation of brain tumours.

the initial placing of the original contour is very important. A wrong placing may result in too little of the desired object being segmented or additional objects being segmented.

Level sets have been applied to segment various parts of the human body. For example, [Droske et al., 2001] used level sets to segment brain tumours in MR image slices. The results of his experiments are very close to what an expert in the field can obtain, as shown below in Figure 2.10. The top images are evaluated by an experienced neurosurgeon while the bottom ones are segmented by the level set algorithm.

[Yang et al., 2008] incorporates statistical region information into the basic level set model to improve the robustness of the segmentation of medical images. This improve the accuracy of segmentation for images with weak or fuzzy edges. Similarly, [Chen and Tseng, 2008] makes use of statistical information in the form of Bayesian risk hypotheses to perform segmentation on noisy or low-contrast images. A review of level set implementations which incorporate statistical information was performed by [Cremers et al., 2007]. While more ro-

bust than the basic form of level set, these implementations suffer from the need to extract information from training samples. It may be difficult to obtain training sets of sufficient size and variation to extract meaningful statistical data.

2.2   Atlas-based Segmentation Methods

After looking at the common techniques used for segmentation, the next step would be to review the two main types of atlas-based segmentation. Atlas-based segmentation is a more sophisticated category of segmentation techniques which makes use of prior domain knowledge and additional information about the data to improve the accuracy of the segmentation. These can include shape and intensity data as well as spatial information of the relative locations of various objects in images. The use of such data can improve the accuracy of segmentation by reducing the number of false positives. It can also potentially reduce computation time by making the algorithm converge to the solution faster.

As mentioned previously in Chapter 1, atlas-based segmentation methods can be broadly separated into two broad categories. These are the probabilistic and non-probabilistic approaches. A probabilistic approach can be defined to be an approach which incorporates statistical data derived from a set of training samples to drive the segmentation process. On the other hand, a non-probabilistic approach makes use of information derived from a single image. Each approach has its own merits and disadvantages, which will be looked into in the subsequent sections.

2.2.1   Probabilistic Atlas-based Segmentation Methods

Probabilistic atlas-based segmentation methods make use of statistical information derived from training samples to guide the algorithm towards the global minima. This statistical information is derived from various features of the training data, including shape, intensity, edge locations as well as other information derived from these features. The statistical information is then incorporated into an optimization function which will make use of the

information to guide the segmentation. Also, the statistical information can be used to cluster pixels into groups representing separate objects. This is done by comparing the features of a target pixel with the information gathered from the training samples.

The advantages of using probabilistic atlas-based segmentation techniques is that they can be very robust and can definitely find the global minima if the global minima is located within the range spanned by the training samples. However, it is very difficult to determine if the training set includes all possible variations of the objects of interest. Increasing the number of training samples would help resolve this problem, but determining the amount of training samples required is also none trivial. Also, in many cases, it may also be difficult to obtain enough training samples to effectively use a probabilistic approach.

Nevertheless, probabilistic atlas-based segmentation methods are widely used in medical image analysis applications.One method of segmentation is through the use of Active Shape Models (ASMs). ASMs are a parametric deformable model which uses a point distribution model (PDM) to fit a model to a target [3]. A PDM is a statistical model built from a set of training samples via Principle Components Analysis (PCA). The features used are usually the edges which define the areas of interest, or control points which define the shape of the objects. Similar to ASMs are the Active Appearance Models (AAMs) which are a generalization of ASMs. AAMs make use of all the information in the image regions, unlike ASMs which only use information near the defined points[4].

ASMs and AAMs have been used segmenting a wide range of body parts. A lot of work has been done on the brain, heart, liver, kidney and bone. [Cootes et al., 1994] published a review of ASM and AAM techniques used in brain segmentation. [Wang and Staib, 2000], [Lötjönen et al., 2004] and [Keleman et al., 1998] proposed algorithms for medical image segmentation using ASMs, while [Mitchell et al., 2001] used a hybrid AAM/ASM deformation algorithm to segment the left and right ventricles of the heart.

Another approach which makes use of statistical models for segmentation is to use the

---

[3]http://www2.imm.dtu.dk/ aam/downloads/asmprops/asm.html
[4]http://bagpuss.smb.man.ac.uk/ bim/Models/aam.html

knowledge acquired from the training samples to perform classification of the pixels in the target. This classification can be for all pixels in the target, or just those near a deformable contour. In the former case, the end result of the algorithm would be similar to that of a region-growing algorithm where pixels belonging to the same object are classified together. In the later case, the classification of the pixels would drive the deformation of the contours.

[Prastawa et al., 2005], [Park et al., 2003], [Xue et al., 2001], [Sluimer et al., 2005] and [Straka et al., 2003b] proposed algorithms which perform segmentation by classifying the pixels in the target images, while [Prastawa et al., 2003], [Al-Zubi et al., 2002], [Bosc et al., 2003] and [Shen and Davatzikos, 2000] used tissue classification to deform a contour.

2.2.2   Non-probabilistic Atlas-based Segmentation Methods

Non-probabilistic methods usually only make use of a single image as the atlas, as compared to probabilistic approaches which often require multiple image sets to create the atlas. Data is extracted from the image, and used to pre-process, initialise and guide the algorithm towards the global minimum.

Non-probabilistic segmentation methods function in a similar way as probabilistic methods. The main difference is in the type of atlas and how they are incorporated into optimization functions. The main advantage of using a non-probabilistic approach would be that only a single image is required to perform the segmentation. In many cases, it can be difficult to obtain data sets of sufficient size to do probabilistic segmentation. On the other hand, one disadvantage of a non-probabilistic approach would be that it is not as robust as a probabilistic approach. This is because the amount of domain knowledge that can be extracted from a single image is definitely less than what can be extracted from a set of images. The end result is that there are fewer constraint's on the deformation, increasing the chance of the algorithm getting stuck in a local minima. However, not all problems require the level of robustness given by a statistical model. Also, robustness can also be built into the optimization function itself rather than the atlas.

[Chen et al., 2003], [Bondiau et al., 2005], [Dawant et al., 1999], [Hartmann et al., 1999], [Cuadra et al., 2001], [Cuadra et al., 2003] and [Cuadra et al., 2004] proposed non-probabilistic segmentation algorithms which utilize the Demons algorithm to register the atlas contour to the target. The Demons algorithm uses the concept of optical flow commonly used in tracking algorithms to compute forces between the atlas and the target[5]. These forces are then used for generating a deformation field. Assumptions made when using algorithms based on optical flow is that the images should be of the same modality and have similar intensity distributions.

[Shen et al., 2001], [Shen et al., 2004] and [Ding et al., 2005] employ active contours in their algorithms to guide the deformable contours to their final configuration. One advantage of using active contours is that they have an implicit regularization function unlike the Demons algorithm. Level set based algorithms are similar to active contours in the sense that Level sets can be used to guide a deformable contour. The main difference would be that level set algorithms can allow for changes in topology which is not so easily achievable with a normal active contour implementation. Level sets and active contours will be discussed in greater detail in subsequent sections. [Vemuri et al., 2003], [Duay et al., 2005] and [Baillard et al., 2001] are examples of proposals which make use of Level sets for deformation of the contours.

2.3 Segmentation of the Liver

Medical image segmentation has been applied to many parts of the human anatomy. The algorithm in this paper is able to segment most parts of the body as long as the appropriate atlas is supplied. However for a start, the liver and abdomen were chosen based on availability of data and the importance of segmentation for the treatment of liver ailments.

Much work has been done in the area of segmentation of the liver. Some examples of algorithms developed for liver segmentation include [Massoptier and Casciaro, 2007] who proposed a graph-cut method for automatic segmentation of the liver, and [Martin et al., 2004] who developed a semi-automated framework for the segmentation of the liver as well as tu-

---

[5]http://www.itk.org/pipermail/insight-users/2004-July/009384.html

mours and blood vessels in the liver. [Chen et al., 2009], [Lee et al., 2007], [Liu et al., 2005] and [Okada et al., 2007] are other examples of algorithms for the segmentation of the liver.

Chapter 3

Problem Formulation

As mentioned in the motivation, there is a need to create a system that allows the hospital to perform in-house segmentation, quantification and visualization of organs in CT images. The basis of such a system is the accurate segmentation of the organs in CT images along with their sub-components and the blood vessels running through and around them. Once that is done, an accurate three dimensional model of the organ can be reconstructed. Quantification and visualization can then be done based on the model.

In order to better understand the requirements of the project, a proper problem formulation is required. This includes detailed and in-depth analysis of the required inputs and the desired outputs.

3.1 Input Analysis

In any atlas-based segmentation algorithm, the main inputs would be the atlas as well as the data samples for segmentation. Good knowledge of the input and the information that is provided by it is an essential step in obtaining a good understanding of the complexity of the problem. There are two components for input analysis: the model characteristics and the input data characteristics.
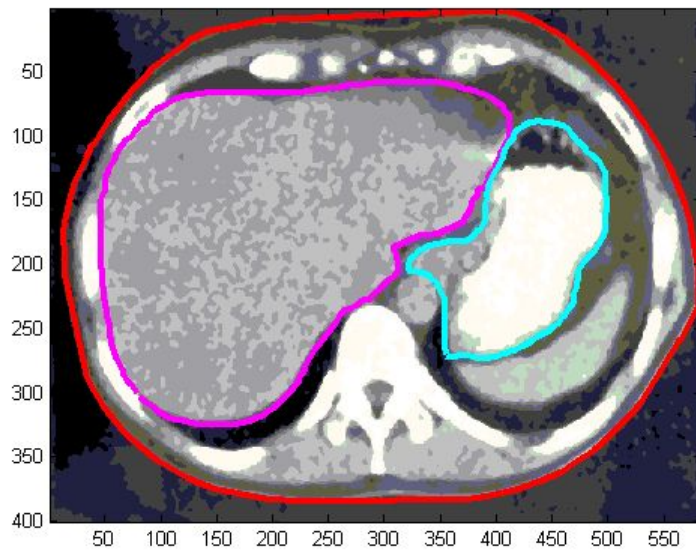
Figure 3.1: Diagram showing an atlas

3.1.1 Model Characteristics

The model used in this project is a single CT image in which the major areas of interest have been clearly delineated. Currently, these areas are the stomach and the liver. As can be seen from Figure 3.1, the contours of the areas have been drawn out, and these will be deformed to fit their respective areas in the target CT images. More details on what information is extracted from this model to be used in the algorithm is present in Chapter 4.

3.1.2 Input Data Characteristics

The input data for this project are abdominal CT images. This modality is widely used in medical treatment for abdominal ailments. Furthermore, there are several properties of using such images that make using such data for segmentation both interesting and challenging.

One advantage of using CT data as opposed to other forms of medical imagery is that all body parts are shown clearly in the images and there is no overlapping of any two body parts. This is unlike other modalities such as X-ray imaging, where the overlapping of tissue
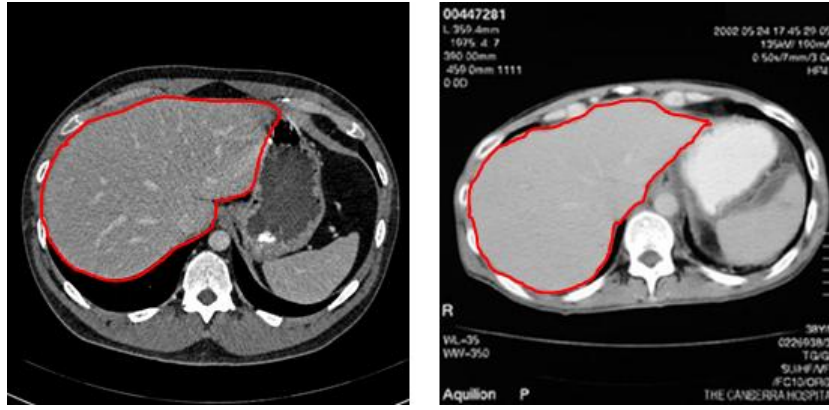
Figure 3.2: CT images from two different datasets, illustrating the amount of variation between different individuals

is always present. As such, using CT images simplify the segmentation task due to the reduced amount of inherent fuzzy regions.

However, there are still many challenging aspects to the use of CT images for segmentation. These help to define the requirements the project must fulfill in order to perform its task of segmentation well.

Shape Variation of body and body parts

The shape of a healthy human is approximately the same across different specimens, except for some differences in the shape and size. This means that while the shape of the abdomen of two individuals may be similar, there will likely be some obvious differences. Not only will the external body shape be different, the shapes of their internal body parts are likely to exhibit some differences as well. These variations will be reflected in the CT data. This is shown in Figure 3.2 which features a comparison of the differences in shape of the liver from two different datasets. As such, any segmentation algorithm must be able to handle such variations in shape.

Furthermore, this project aims to create a robust segmentation technique that can make use of data from a single 2D atlas to segment multiple slices of CT images. As such, the
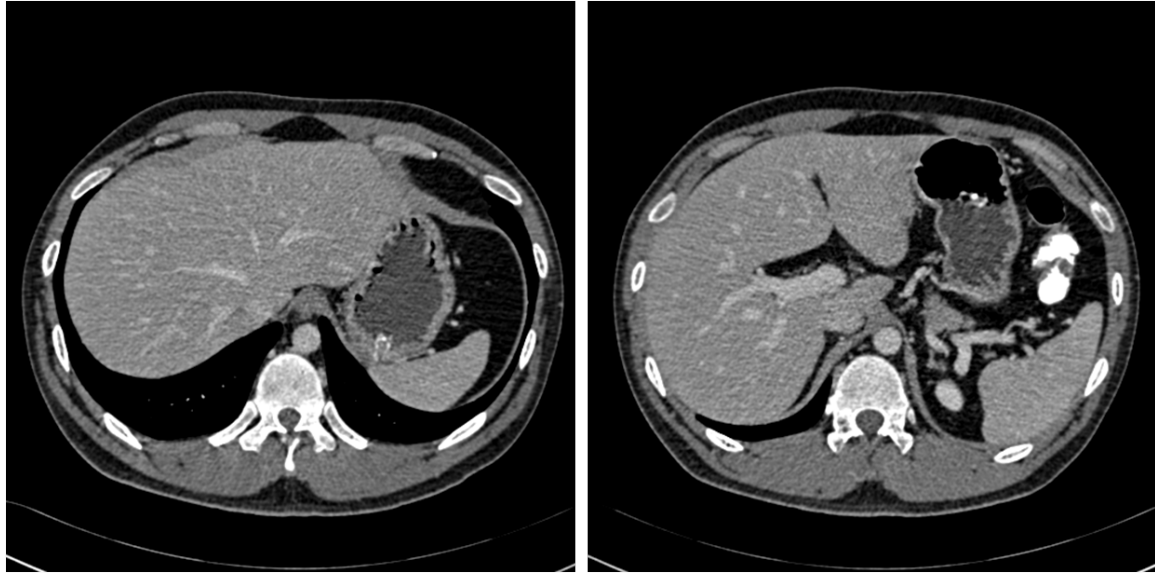
Figure 3.3: CT images from the same dataset, but at different slice

shape variation of the regions of interest at in different slices of the same dataset is also an important factor to consider. As can be seen from the livers in Figure 3.3, this variation can be very significant.

Intensity Variations

Intensity variations between different CT datasets occur due to the use of different scanners as well as the time of data acquisition. Various contrast enhancements which are used to make certain features more prominent are yet another contributor to the intensity variations across images. Figure 3.2is an example whereby the image on the right is relatively brighter than the image on the left. Furthermore, the stomach contents show up very brightly in the image on the right, whereas it is much darker in the image on the left. A segmentation algorithm must be robust to such variations.

Texture and Artifacts

This project seeks to segment various body parts in the abdomen. One thing that complicates this is the presence of other body tissue within the target regions. An example of this
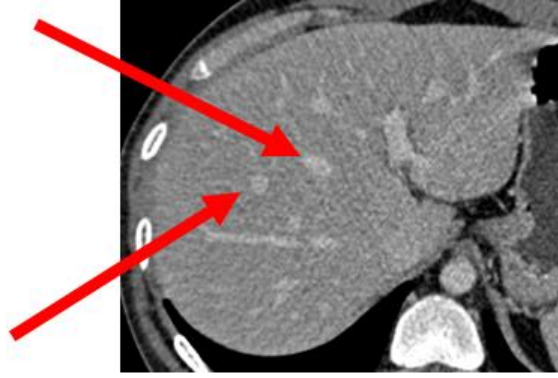
Figure 3.4: Diagram showing blood vessels in liver pointed out by the red arrows

is the blood vessels within the liver, pointed out by the red arrows in Figure 3.4. The presence of these noise features will add to the complexity by adding false positives to the results.

Another source of noise features are the artifacts created in CT images due to phenomenon like partial volume effects and beam hardening. These phenomena generate false features in CT images which may even fool experienced practitioners. Therefore the algorithm must be robust enough to handle the presence of such features, or a method must be found to remove them.

Poorly Defined Edges

While there are no overlaps in CT imagery, there are still problems with poorly defined edges in the images. This is mainly caused by the similarity of the tissue intensity within the CT image. As such, there may be a lot of broken edges as well as spurious edges resulting from noise. This is illustrated in Figure 3.5 in which the contours around organs in the edge maps are often not closed loops. These poorly defined edges adds to the complexity of the problem since without edges, the algorithm may be led to a wrong edge, resulting in poor segmentation.
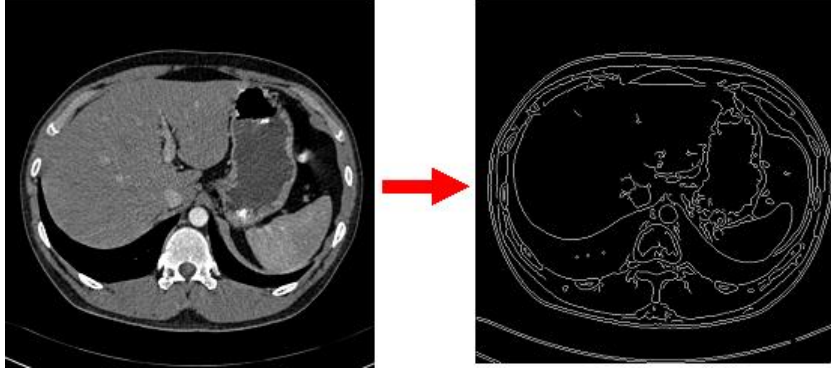
Figure 3.5: A CT image and its edge map. Note the many areas in which the edges are broken

3.2 Desired Output

The desired output of the project are the contours of the various body parts in the abdomen. These contours must accurately segment the various body parts in question and not overlap each other.

3.3 Problem Definition

The solution to the segmentation problem proposed in this thesis can be described in mathematical notation in order to improve the understanding of the requirements.

Inputs:

- Let B = $\{e_k\}$ be the set of edge points in the Image. B contains the edges of the body parts we want, edges of other body parts as well as noise. Some edges of the regions of interest are not contained in B.

- Let C be a set of contours $C_i = \{p_{i,j}\}$ which are the deformable models of the body parts we are interested in.

- Let S($p_{i,j}$) be a function related to shape information.

Output:

- The deformed C, which we call C', which represents the extracted contour of the body parts we want.

Problem Definition:

Define f as a correspondence function from C to B, that is,

$f(p_i) \in B$

Let D(C) denote a deformation function of C by moving the points $p_i \in C$ to new locations

$p'_i = D(p_i)$

Then, the problem is to find the D and f that minimizes the total error E,

$$E = E_p + \alpha E_s \tag{3.1}$$

where α is a weight.

$$E_p = \sum_i ||D(p_i) - f(p_i)||^2 \tag{3.2}$$

$$E_s = \sum_i ||S(D(p_i) - S(p_i))||^2 \tag{3.3}$$

with the constraints that all contours must lie within the contour of the body cavity and no contours must overlap each other. In mathematical terms,

Let C_0 be the contour of the inner body cavity

Then

$$\forall c_i \in C, i \neq 0, c_i \bigcap c_0 = c_i \tag{3.4}$$

and

$$\forall c_i, c_j \in C, i \neq 0, c_i \bigcap c_j = \emptyset \tag{3.5}$$

Chapter 4

Algorithm

The algorithm used in this thesis is an atlas-based registration algorithm which is designed as a multistage pipeline. The atlas provides spatial knowledge of the shape and location of the targeted body parts. It also provides other information which helps improve the quality of the registration. Details on the construction and contents of the atlas are explained in Section 4.1.

The algorithm pipeline consists of five main components. These are:

- Image Preprocessing

- Body Contour Extraction

- Global Registration

- Local Registration

- Collision Management

The collision management component is integrated into the two registration components and serves to constrain those body parts which are near each other. Figure 4.1 illustrates the flow of the algorithm and how the atlas and the collision resolution component interacts with the main pipeline. The atlas is used to initialise the position of the contours and provide feature information that is used for registration of the contours to the image. Collision resolution is run after global and local registration steps in the pipeline, as well as at the end of the algorithm. Further clarification on each component of the algorithm is given in
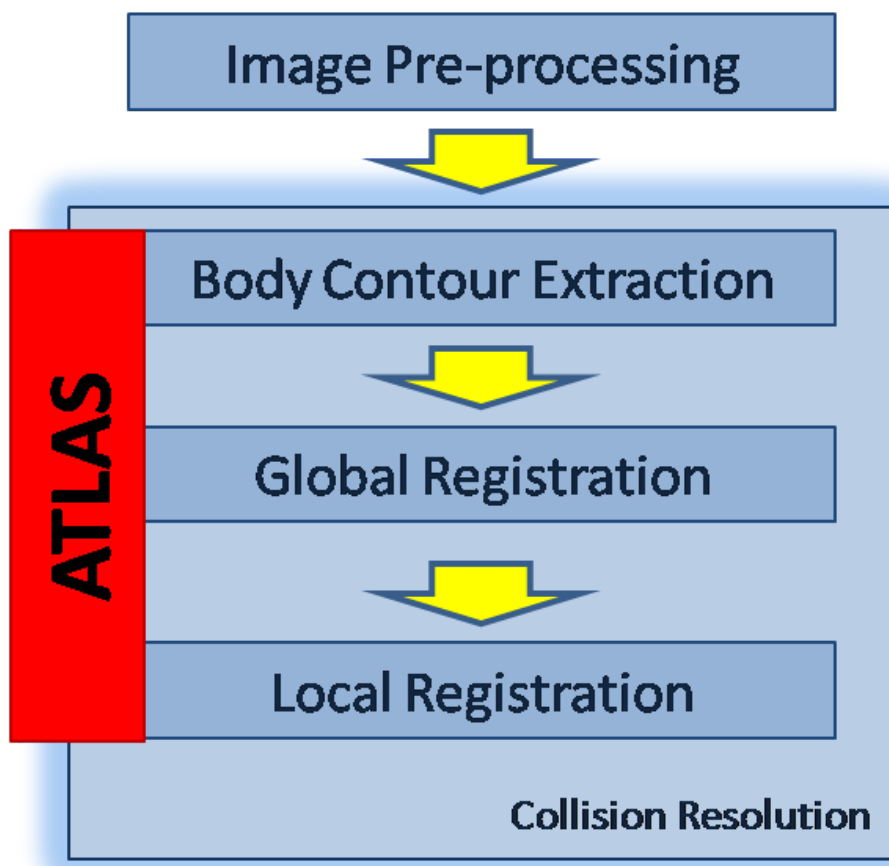
Figure 4.1: Flow Diagram detailing the algorithm used for the registration

Sections 4.3 - 4.6.

4.1 Atlas

There are 3 components to the atlas. They are the:

- Body part contours

- Intensity gradient directions at each point of the contours

- Boolean value to represent the presence of empty space between a point on a body part contour and the centroid of a body part

The body part contours are the principal components of the atlas. They provide the shape and location information of the individual body parts. This helps with both the initialization of the contours on the target images, and the finding of correspondences during the registration phases.

The intensity gradient direction vectors of each point on each contour provides information on the area surrounding the contours. This robust intensity-invariant feature, called an IDD, is a one-dimensional vector running normal to the contour at each contour point. Each element in the IDD stores the direction of the difference in intensity between the current point and the previous point. This information is the primary method of finding the correspondence between each point on the contours and the target image. A pictorial illustration of one intensity gradient direction vector is shown in Figure 4.2. Section 4.13 will give more details on how correspondence is found using this vector.

The last item in the atlas is used mainly to fix the problem of empty spaces within body parts, namely the stomach and liver. These body parts contain dark areas which are mainly body fluids or air pockets. This is illustrated in Figure 4.3, which shows the air pocket in the stomach having the same intensity as the background. Furthermore empty spaces such as this introduce distinct edges into the image which will complicate the registration process. By adding the boolean value to the atlas for every point, the algorithm receives early
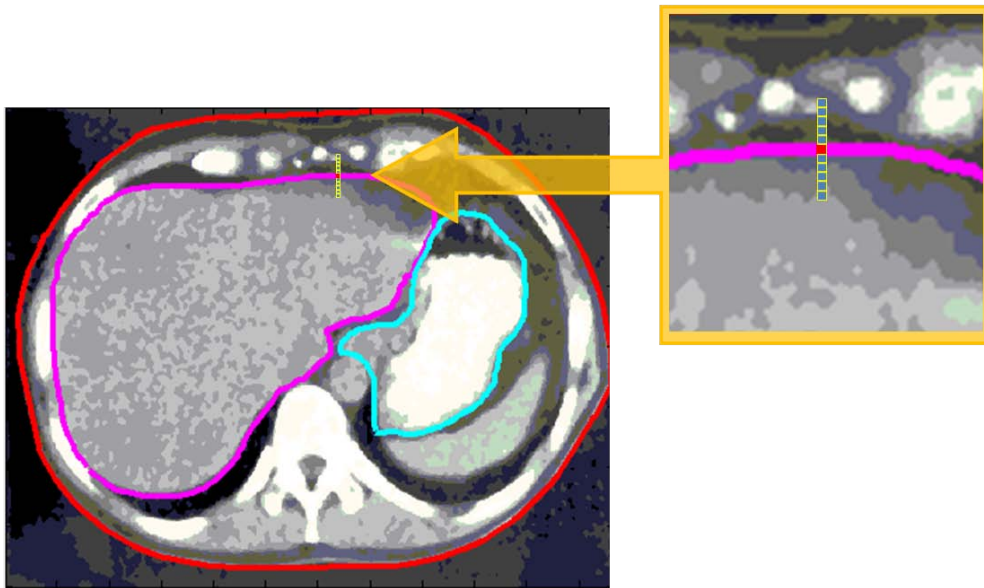
Figure 4.2: Illustration of an intensity gradient direction vector of a point (marked in red) in the atlas
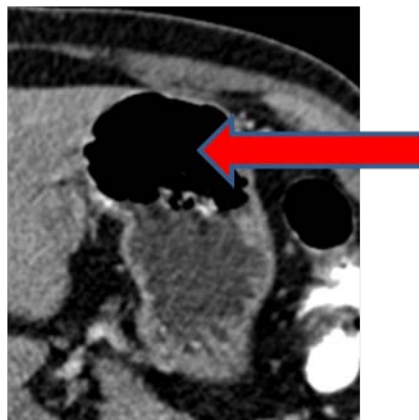

Figure 4.3: Image of stomach showing the presence of an air pocket, which has the same intensity as the background

warning that such spaces exist in that vicinity and will hence include that in the contours should they come across one.

In the implementation, the boolean value is set to "0" for those points where there is a possibility of an empty space occurring between it's position and the position of the centroid for the body part. Otherwise it is set to "1".

4.2   Image Preprocessing

The first step would be to perform some pre-processing on the target images to remove some objects which appear outside of the body. In general, the main cause of such objects is the bed of the CT machine, which shows up when the CT image is taken. Image preprocessing is also performed to smooth the image. This will improve the quality of the edge detection later.

The reason for performing the image preprocessing step is to extract the outer body contour from the image as those objects lying outside of the body contour will interfere with the algorithm. Smoothing the image will also remove much unwanted information from the CT images, such as the texture of the organs as well as minor blood vessels. These will show up during edge detection and add more false positives later during segmentation.

Two issues can be solved in the image preprocessing phase using a single solution. Notice in Figure 4.4 that the bed of the CT machine shows up as two curves in the CT images, as designated by the red arrows. Being thin lines, they can be easily removed by using a median filter. This is the same for the fine blood vessels and texture patterns inside the body. Median filtering has an advantage over other filters in that it maintains the position of the edges, while the others will add a degree of fuzziness to the position of the edge. Having the position of the edge intact is very important since the goal of this thesis is to segment the organs.
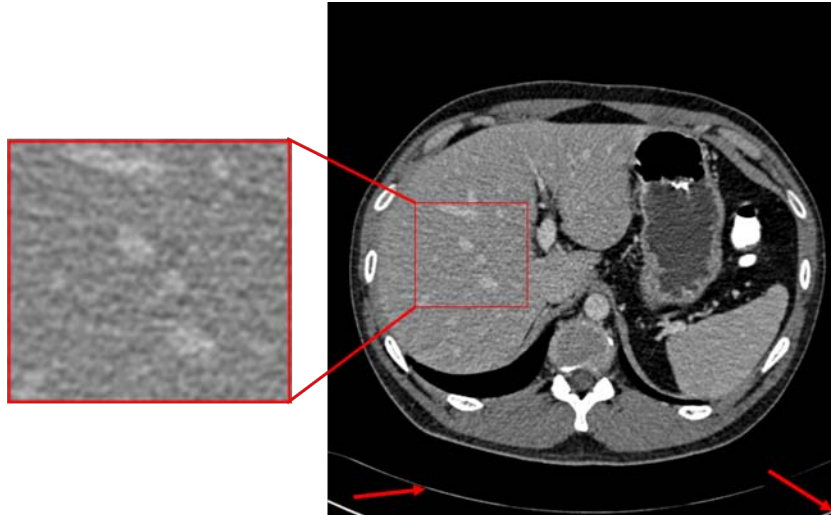
Figure 4.4: Abdominal CT image showing the scanner bed and the texture of the organs which are to be removed

4.2.1 Median Filtering

Filtering is a common technique used as a preprocessing step in image processing to remove noise and other artifacts in images. In filtering, a window is usually taken around a pixel of interest and an intensity value for that pixel is that calculated based on the intensities of the pixels in the window. Of the many types of filtering, mean and median filtering are among the more common techniques used. Mean filters assign the mean value of the intensities within the window to the target pixel, while median filters will choose the median value as the value for the pixel.Another type of filter which is commonly used is the gaussian filter, which calculates the target pixel intensity as the weighted average of the intensities within the window, with the weightages given by a gaussian function. For these various types of image filters, the median filter(Figure 4.5) was deemed the most suitable.

The main reason why median filtering was chosen for the preprocessing step of this algorithm is because median filters have the useful property of retaining edge information within an image. Mean filters and gaussian filters tend to blur the edges in an image. This is because the median filter does not create new unrealistic pixel values when the window lies over an edge, while the other filters will do so. Since the focus of this thesis is to segment the contours of various organs in a medical image, the preservation of edges in the images is of utmost im-

Figure 4.5: An example of a median filter at work. The window size used here is 3 by 3

portance. Figure 4.6 shows the result of applying median filtering to a CT image. The noise and texture were removed while the shapes and edges of the target body parts were retained.
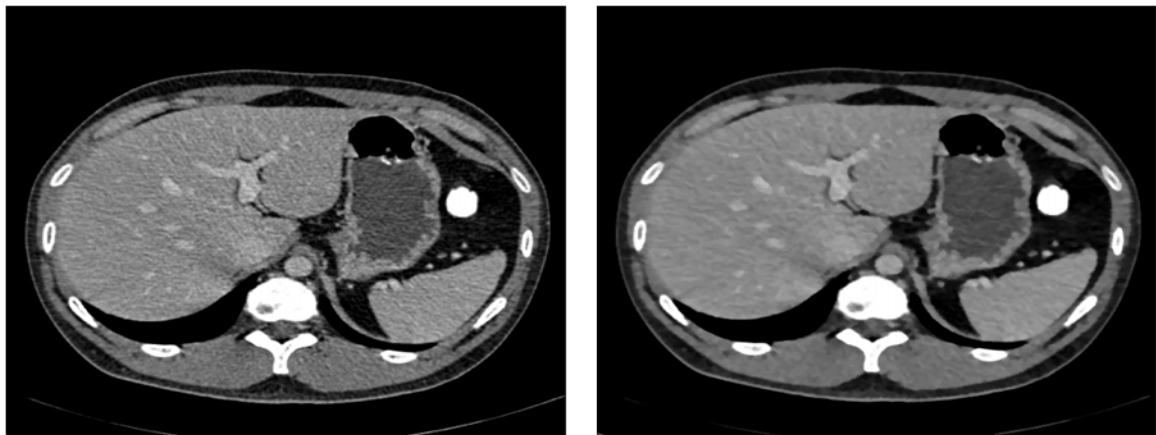
Figure 4.6: Results of median filtering (right) applied to a CT image (left)

4.3 Body Contour Extraction

The outer body contour is needed to align the model and the target image into the same coordinate space. This problem is solved by finding the convex hull of the body in both the model and the target image. This is because the outer body contour is almost entirely convex, and thus, finding the convex hull will give a good approximation of the outer body contour. In fact, it was observed via empirical experimentation that even if two objects are not entirely or mostly convex, as long as they are of similar shape, their convex hulls would

Figure 4.7: Sample images showing a cloud of points(left) and the resultant convex hull(right)

work as well for the purpose of global alignment.

4.3.1 Convex Hulls

The convex hull is a very useful tool as it captures the rough shape and extent of the data set. The convex hull C of a set of points S is the smallest convex polygon that contains all the points of S. This is illustrated in Figure 4.7. It can also be defined as intersection of all convex sets containing S.

Mathematically, it can be given by the expression:

$$C = \{\sum_{j=1}^{N} \lambda_j p_j : \lambda_j \geq 0 \quad \text{for all } j \in \mathbb{N}, \sum_{j=1}^{N} \lambda_j = 1\} \tag{4.1}$$

The convex hull function in MATLAB uses the Quick Hull algorithm [Barber et al., 1996] to determine the convex hull of the body in the CT image. This algorithm is included as parted of the Qhull package[1]. The Quick Hull algorithm uses a divide-and-conquer method which is based on the observation that the points in the dataset can be split into two sets recursively, with the algorithm working on one set while temporarily ignoring the other. In a balanced dataset, where all the points are spread across the space, Quick Hull requires only $O(NlogN)$ time.

---

[1]http://www.qhull.org

Additional computation is done to prevent the inclusion of the CT machine bed in the convex hull. This is done by rejecting edges in the convex hull found that are too long. Observation shows that the body contour is approximately elliptical and hence any edges in the convex hull should be short. Rejecting these long edges improves the accuracy of the body contour extraction.

Figure 4.8 shows the result of naively applying the convex hull algorithm to the CT images. It is clear that the noise and spurious edges in the images resulted in an inaccurate segmentation of the outer body contour. After refinement, the segmentation is much more accurate, as can be see from Figure 4.9.
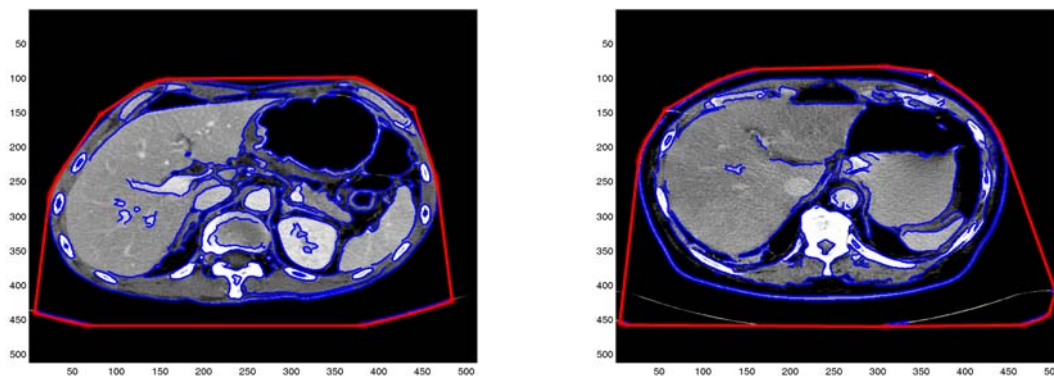
Figure 4.8: Results of applying convex hull to CT images without rejection of long edges. Note how the convex hull include noise points outside of the body contour.

4.4 Global Registration

After segmenting the body contour from the CT image, the atlas is brought into the coordinate space of the target in the global registration step. Using this as the first level of initialization, the possibility of the algorithm being trapped in a local minimum is reduced.

The Iterative Closest Point algorithm(ICP) is used to register the two objects. This is performed on the outer body contours of the atlas and the target.
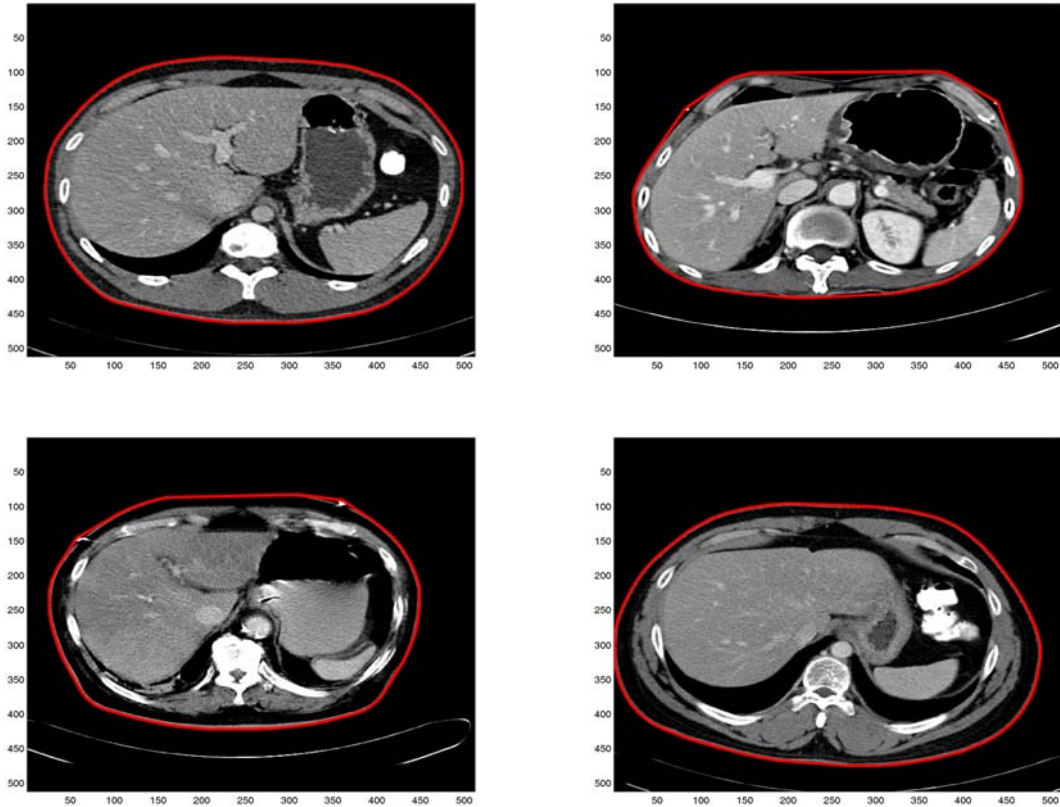
Figure 4.9: Results showing body segmented from image using convex hull algorithm with iterative rejection of long edges. Noise points are now excluded.

4.4.1 Iterative Closest Point

ICP was introduced in 1992 by [Besl and Mckay, 1992] as a means of registering two sets of data points. This is accomplished via the computation of a transformation matrix using the displacements of each point in the model set to it's closest corresponding point in the reference set. ICP is easy to implement and will generally provide good results. However, it requires a good initialization as it can be trapped in local minima.

The implementation of ICP used in this project is coded entirely in MATLAB. It comprises of three main components:

1. determining the correspondence between the atlas and the target

2. calculating the transformation matrix based on the correspondence
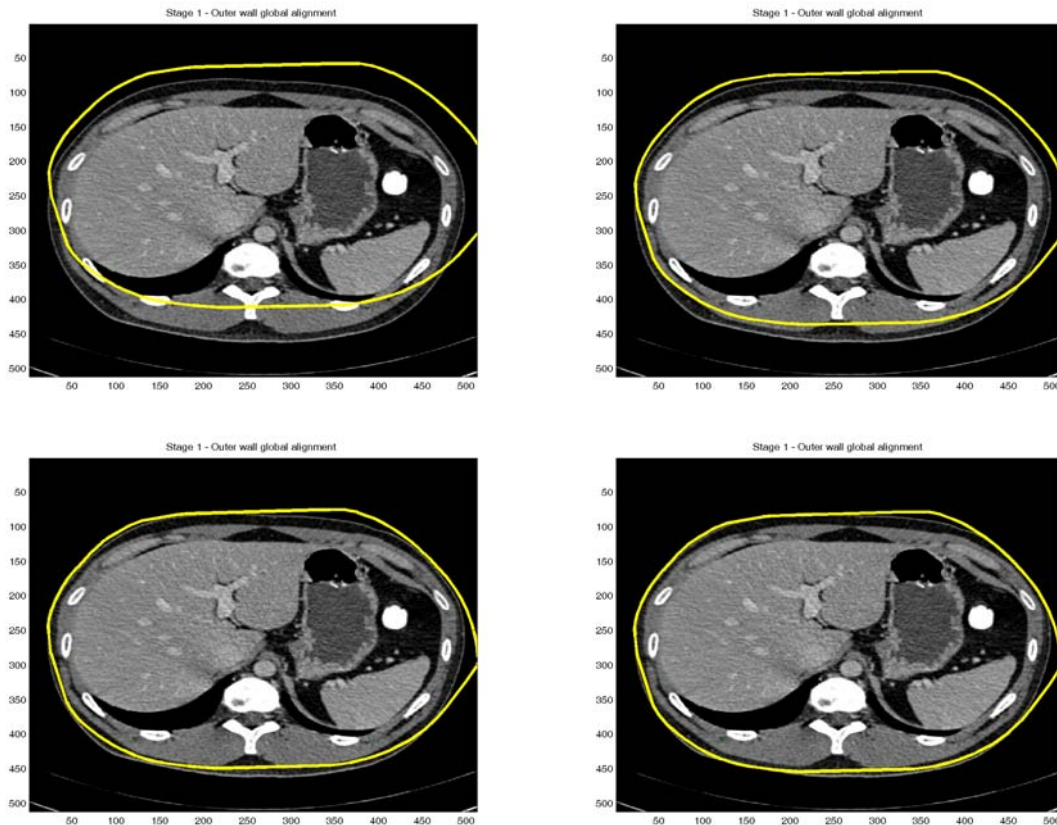
Figure 4.10: Image sequence showing the global registration via ICP

3. transforming the atlas to its new configuration

The algorithm was based on mathematical formulae from lecture notes by Dr Leow Wee Kheng of the National University of Singapore[2]. It also included a K-D tree implementation written by Guy Shechter[3] which was used for determining the closest point correspondence efficiently. The distance measure used is Euclidean distance.

Figure 4.10 shows an atlas contour being registered to the outer body contour of a target image. As can be seen, the registration is very fast and takes about four to six iterations on average. This is mainly due to the simplicity of the objects being registered.

---

[2]http://www.comp.nus.edu.sg/c̃s6240
[3]http://mathworks.com/matlabcentral/fileexchange/loadFile.do?objectId=4586&objectType=file

4.5 Local Registration

After the global registration step, a local alignment step is still necessary to bring the contours in the atlas as close as possible to the desired areas in the target image. This is because the variations across patients in terms of organ size, shape and location can be rather significant, making it unlikely for the algorithm to get close to the desired solution with just the global registration step.

The local registration is done in two steps: A local affine registration of the contours to shift them into position, and an iterative deformation to bring the contours as close to the desired edges as possible.

4.5.1 1st step Local Registration

The first step in the Local Registration stage is to shift the contours closer to the target body parts. This is a similarity transformation where the general shape of the contours is retained. The purpose of doing this is to reduce the possibility of the subsequent deformation stages being attracted to the wrong edges.For this local registration stage, the Iterative Corresponding Points technique proposed by [Ding et al., 2005] is used.

Iterative Corresponding Points

This technique is an iterative optimization process which uses IDDs to determine the correspondence between the model contour and the edge image. As mentioned before in Section 4.1, an IDD is created for every edge point in the atlas. Similarly, in the Iterative Corresponding Point stage, IDDs are calculated for every point in the registered contours. These target image IDDs are much larger than the ones in the atlas. This is because correspondence is determined by comparing each point of the target image IDD with the atlas IDD. The point with the best match is deemed the corresponding point in the image for the atlas point.

Figure 4.11 shows the IDD vector for a single point on the liver contour, and the area it searches for its closest match. Figure 4.12 presents a graphical representation of how corre-

Figure 4.11: Image showing the IDD vector from the atlas and its area of search in the Iterative Corresponding Points algorithm
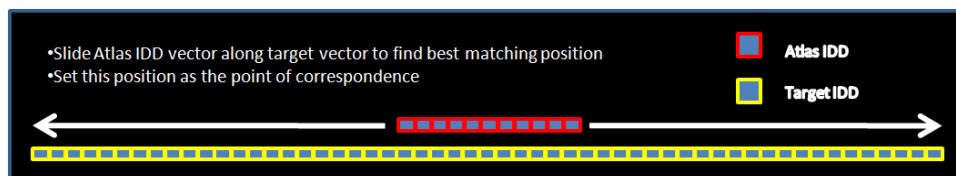

Figure 4.12: Illustration of how correspondence is found in the Iterative Corresponding Point algorithm. The atlas IDD (red) searches along the length of the target IDD(yellow) for the point with the best match, and returns this as the displacement for the current iteration

spondence is found. The method for determining the similarity is Euclidean Distance. After the correspondence is determined, the data is used to calculate a similarity transform which will bring the model closer to the target.

Figure 4.13 shows the registration of a stomach contour to its target in the image. This process is very fast and the algorithm takes approximately 10-12 iterations to converge.

4.5.2   2nd step Local Deformation

After roughly aligning the atlas to the target image, the contours of the various components of the atlas are deformed to the shape of the objects of interest in the target image. This is to bring the contours as close as possible to the desired edge before the final refinement step.

The method used to deform the contours is derived from active contours, a commonly used algorithm for tracking in videos and segmentation of objects in images. The original active contour, while adequate for final refinement of the contour, is ill-equipped to perform the second step local deformation. This is because the atlas contours are still relatively far from their desired configurations, so that possibility of the snake being trapped in a local minima is still very high. Active contours make use of the edge energy in images to determine the direction the contour is to move. Furthermore, a method know as Gradient Vector Flow helps active contours move towards concave contours. However, active contours deform based purely on edge information from the images, hence there is a chance for them to adhere to the wrong edges. A summarization of active contours and its well-known GVF variant is given in Sections 2.1.5 and 2.1.5.

Active contours with GVF is used as the final step in the segmentation of the body parts to refine the results and make the contours smoother. Despite the fact that snakes are easily attracted to the edges of other body parts, it is safe to use it at this stage as the local deformation, which will be detailed in the next sub section, has already brought the contour extremely close to the desired edges.
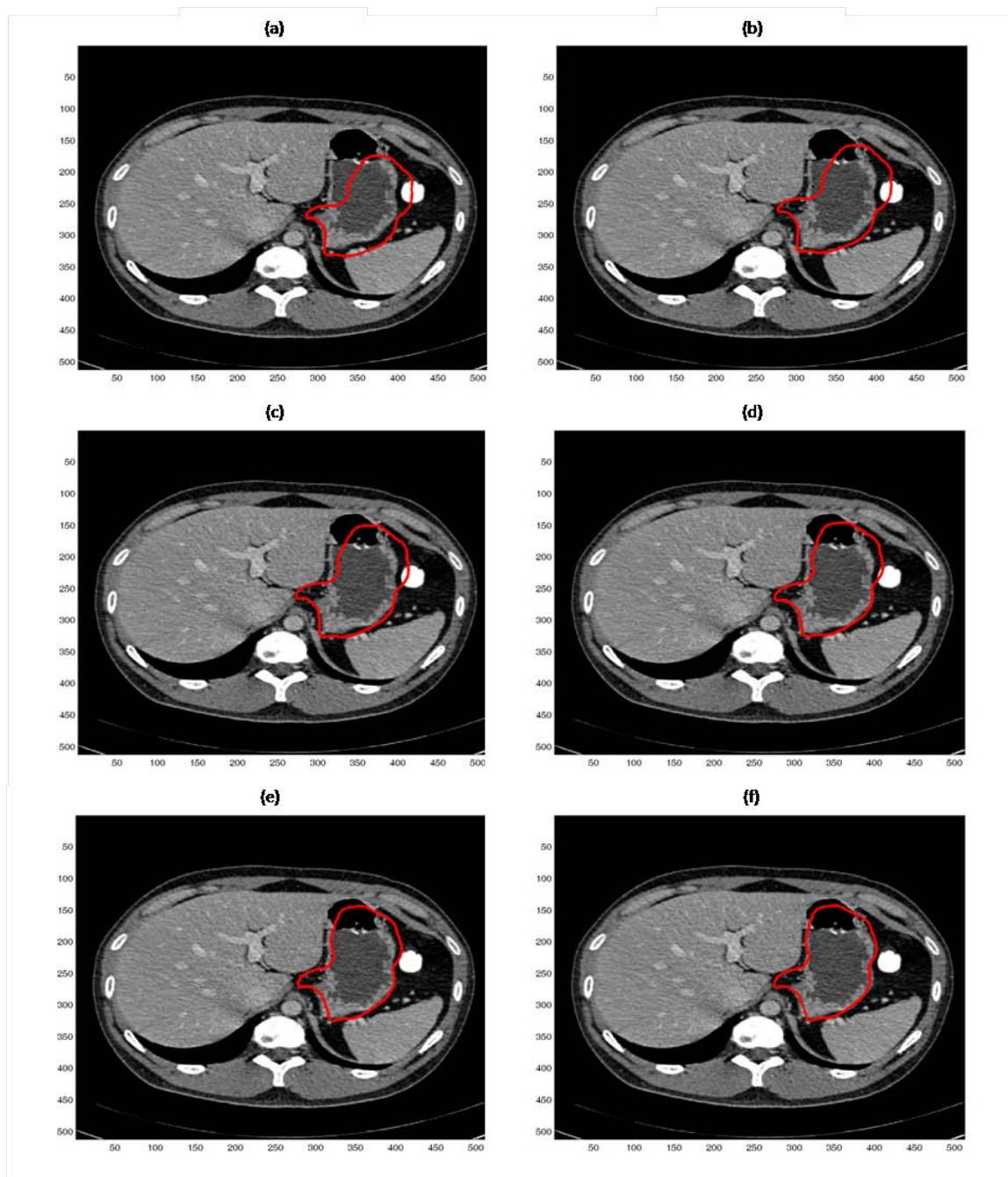
Figure 4.13: Image sequence showing the application of Iterative Corresponding Points on the stomach contour

Iterative Corresponding Snakes

While GVF solves the problem of the snake algorithm not deforming into concave regions, there is still a need to solve the algorithm's tendency to attract to the wrong edges. This issue is primarily the result of the snake algorithm not using all the information that is available from the atlas. The snake only uses the edge information to perform it's deformation. A lot of other information such as shape of the body part and the intensity gradient at each point on the contour is ignored. In order to incorporate such information into the snake, a hybrid of Ding's Iterative Corresponding Points and the snake algorithm is created. This algorithm makes full use of the information in the atlas via the IDD vectors, and retains the internal energy term of the snake as a regularization force. This hybrid method, henceforth known as Iterative Corresponding Snakes, can locate the body part of interest in the midst of all the other edges from other body parts.

In order to understand how the hybridization was achieved, it is necessary to revisit the GVF snake. It was mentioned in Section 2.1.5 that the GVF force directly replaces the gradient vector field of the original snake as the external deformation force. In the Iterative Corresponding Snakes algorithm, the same approach is taken. The IDD correspondence algorithm finds a matching point in the target image for each point on the contour. The direction vector is then weighted and taken as the external force acting on that point. This is then put into the snake algorithm which calculates the deformation of the contour. Figure 4.14 shows an image sequence of the stomach contour with the Iterative Corresponding Snakes algorithm running.

In addition to using Iterative Corresponding Snakes to control the deformation of the inner body cavity contour, an additional curvature constraint was added to control the shape of the body cavity contour. This is because the edge of the body cavity is very poorly defined due to many organs being located very close to it. Having the shape constraint will help prevent the contour from snapping to the wrong edges. This curvature constraint was adapted from the one used in [Chen et al., 2005]. Further details on how this algorithm works can be found there.
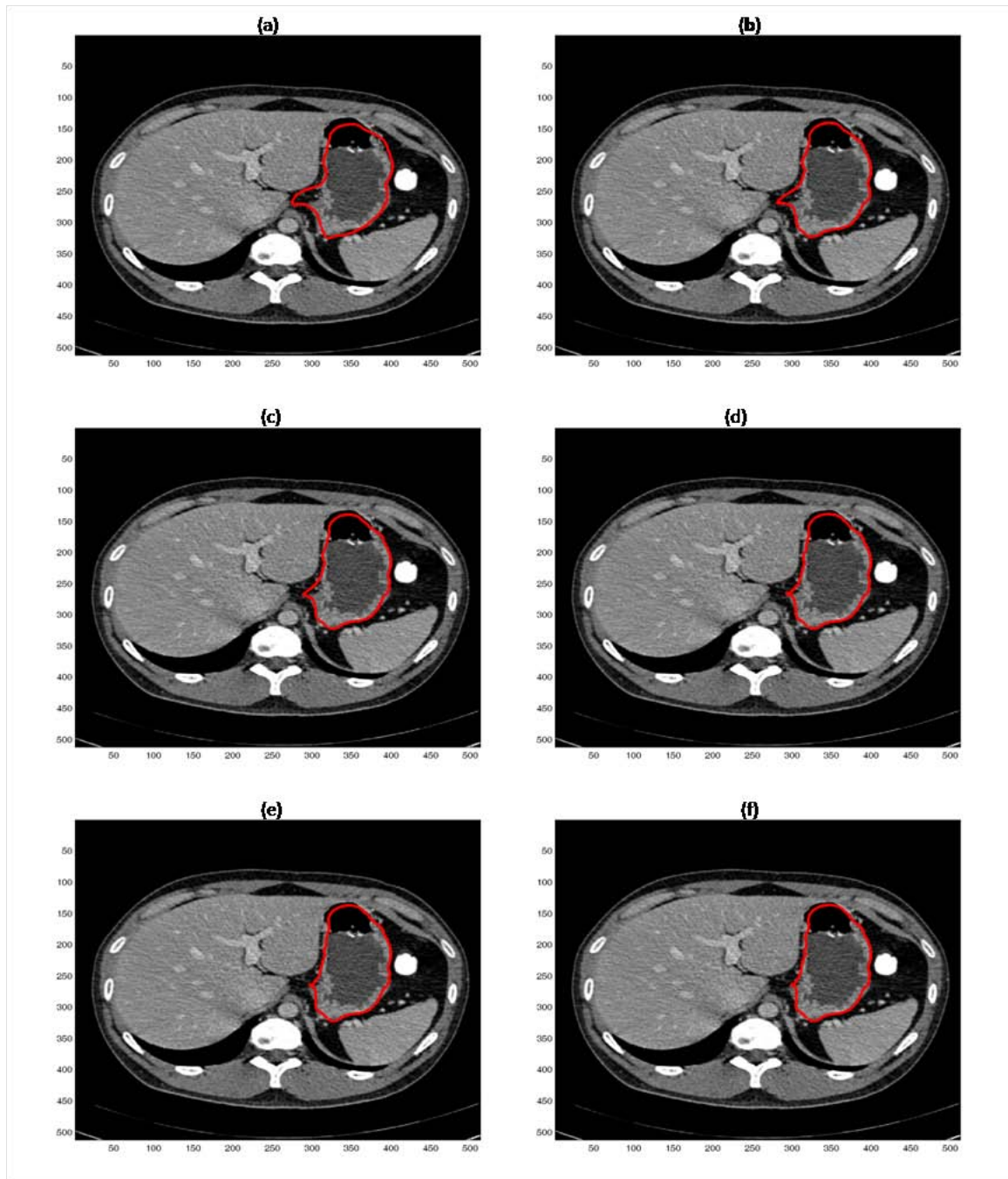
Figure 4.14: Image sequence showing the application of Iterative Corresponding Snakes on the stomach contour

4.6   Collision Management

When the atlas only contains a single contour, the steps up till Section 4.5.2 is sufficient to obtain a fairly accurate registration. However, if more than one contour is present, there is a need to ensure that no two contours overlap. This is a real problem when performing registration with multiple contours. Collision management is required to constrain the contours from overlapping, and a look at the target data reaffirms this need.

The organs in the human body are situated very close to each other. This is especially true for the liver and the stomach, which share a very long common edge. Since the contours for these organs are registered to their targets independently, there is a high risk of the contours overlapping each other. This is unacceptable since in reality, these body parts are separate. Therefore, a collision detection and resolution algorithm is employed to ensure the contours do not overlap. It also serves to guide the contours to their correct positions.

Collision detection and resolution is used throughout the various stages of the registration. However, it is used most intensively in the final refinement stage. This is because the initial stages of the algorithm are primarily for bringing the contours close to the objects of interest. It would not be wise to alter the shapes of the contours too much at these stages as that might result in loss of spatial information and affect the accuracy of the result. However, at the final refinement stages, the contours have already been placed, and the shape information have already played their parts. Therefore collision resolution can be used in conjunction with the refinement process to improve the quality of the registration.

In this thesis, two contours are defined to be overlapping if there is at least one point in one contour which lies within the contour of the other contour. It is however alright if they lie on exactly the same point.

Collision Detection

The detection of collision between 2 contours is done by casting the 2 contours as polygons and performing a point-in-polygon check. In this check, the points in one contour are checked
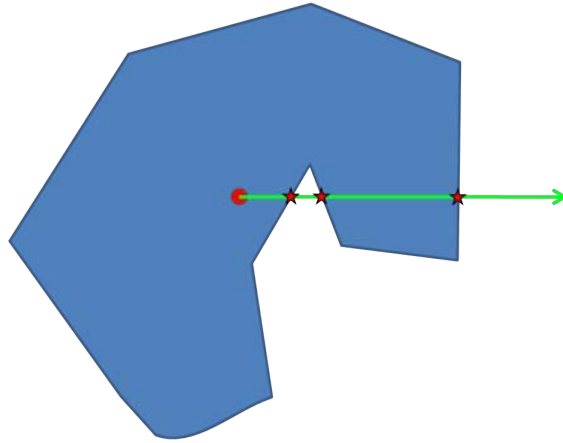
Figure 4.15: Diagram showing the number of crossings of a point inside a polygon. The crossings are denoted by stars.

to see if they lie in the other contour. This is done via the Crossing Number algorithm. This algorithm is based on the observation that a point in within a polygon if a straight line passing through the point crosses the boundaries of the polygon an odd number of times. This is illustrated in the Figure 4.15.

The only exception to this is when the line touches the polygon at one of its apexes. This exception is handled by having the algorithm double count all vertices whose edges lie on the same side of the line.

Figure 4.16 shows the detection of collision points by the collision detection algorithm. Using this information, the collision resolution step can then shift those points until the collision is resolved.

Collision Resolution

Upon detection of a collision, the overlap is resolved by having the points in collision pull away from the other contour. This is done by having the points move a small amount along their normals towards the centre of their own contours. The magnitude of move is weighted by the area encompassed by the contours, so that contours surrounding a smaller area will

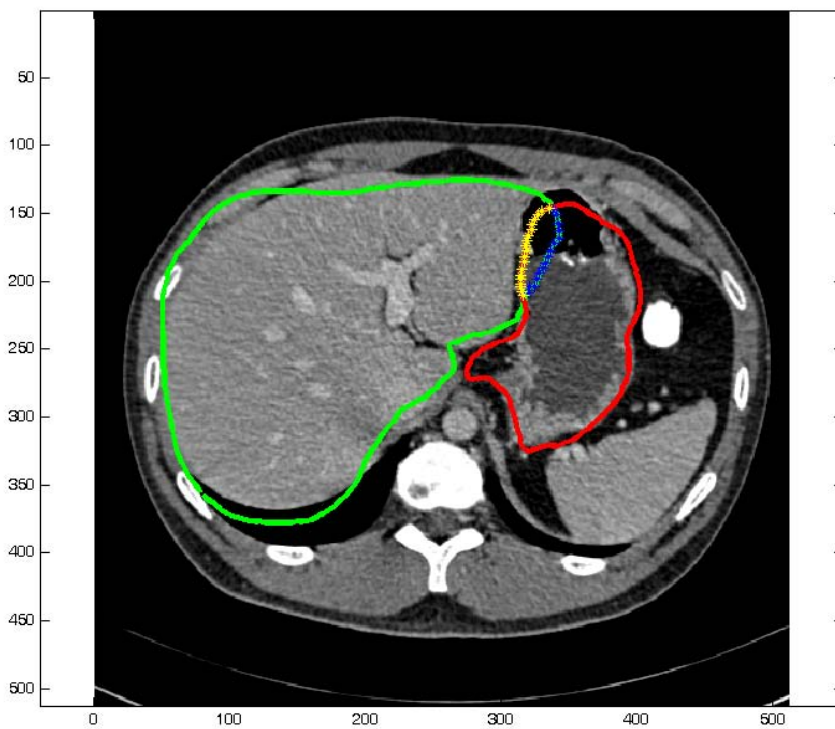Figure 4.16: Image showing the liver(green) and stomach(red) contours with the points in collision denoted in blue and yellow respectively.
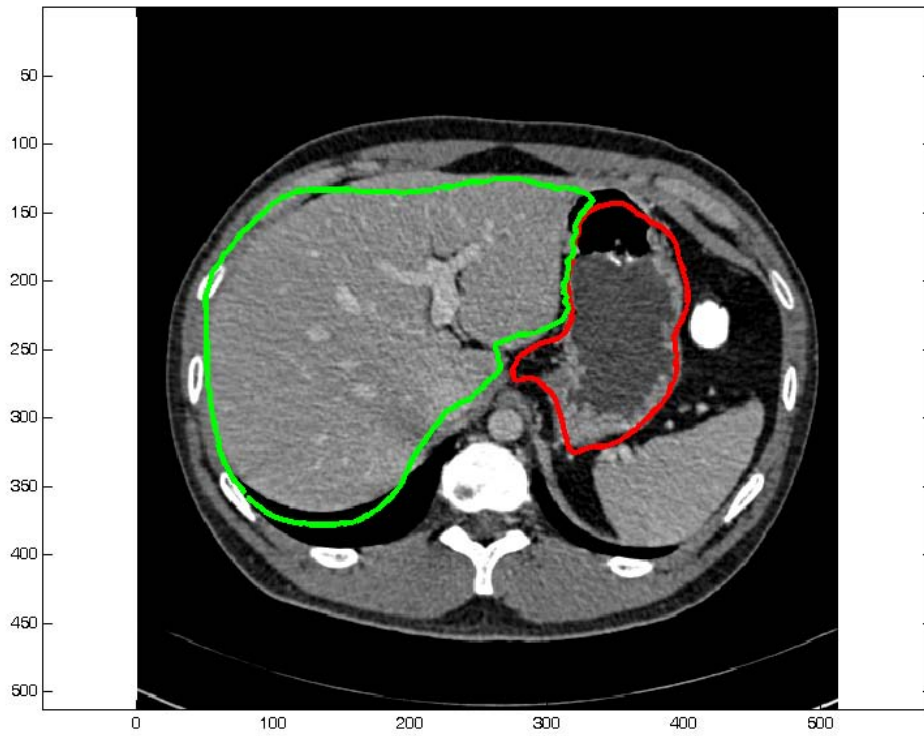
Figure 4.17: Final result after completion of collision resolution

deform less.

Figure 4.17 shows the final end state after the completion of the collision management algorithm. It can be observed that overlap no longer exists, which the two contours just touching at the most.

Chapter 5

Testing and Evaluation

In order to verify the correctness of the algorithm, it is subjected to a series of tests with various data sets and parameters to verify its accuracy and robustness.

Three tests were conducted. The first test was a test of convergence to show that the algorithm will converge to the correct objects. The second test verifies the accuracy of the algorithm by comparing the results with a manually obtained ground truth. Finally, the third test determines the robustness of the algorithm by applying it to multiple datasets.

The algorithm is also compared to results achieved by [Ding et al., 2005], whose work is based on the same dataset as this thesis.

5.1   Test Setup

All implementation and tests were conducted on a PC running Windows XP SP2. The CPU is an AMD64 3000+ and the graphics cards is an NVidia 7600GS. The code was implemented in MATLAB and all graphs were generated using Microsoft Excel.

All CT datasets were obtained courtesy of the Department of Radiology of the National University of Singapore Hospital (NUH). These come with varying degrees of resolution and slice thickness. The datasets also come with different intensity weights, so intensity of the

various body parts are non-uniform across the various datasets. The main dataset used in the implementation and initial testing of the algorithm consists of 200 finely sliced CT images of which 31 were used as those were in the region of the atlas. Also another 8 datasets were used for testing of algorithm robustness. These datasets are more coarsely sliced, hence only a few images from each set were usable.

In these tests, only the liver and stomach are considered, as opposed to the work done by [Ding et al., 2005] where the spleen was included as well. This is because the spleen is generally separate from the rest of the body parts and hence not as interesting as the liver and stomach which share a common border in the CT images. The focus is hence put on the stomach and liver in order to emphasize on the multi-contour aspects of the segmentation algorithm

5.2   Convergence

To test for the convergence of the algorithm, one arbitrary target image was selected and the amount of change of the contours was measured and plotted. This is to determine if the algorithm finds a minima and stops the deformation, hence proving that it does indeed converge. Figure 5.1 shows the target image used for this test.

Figures 5.2 and 5.3 plot the amount of change of the contour versus the iteration step. It should be noted that there are several sharp increases in the amount of change along the graphs, and these are associated to the different registration stages in the algorithm. These stages make use of different types of registration, contour information and features, and hence there is always a lot of movement as the algorithm incorporates these new data to improve the registration result. Nevertheless, the amount of change always tends to zero at the end of each stage, showing that the contours will always converge to a stable minima. This is true for both the stomach and liver contours.

Another method of illustrating converge is to plot the degree of match between the contours and the outline of the ground truth. By showing that the error function decreases as
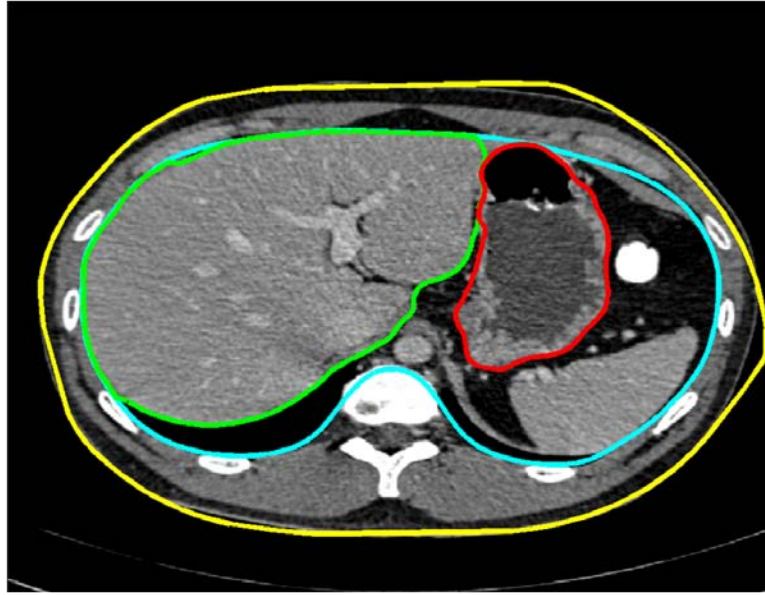
Figure 5.1: Target image used for plotting of graph to test for convergence, with the results of segmentation shown

the contours register to their target, the ability of the algorithm to find the global minima can be deduced. Figure 5.4 shows the target image used in this test and figure 5.5 is the ground truth.

From figures 5.6 and 5.7, it can be seen that both the liver and stomach contours do converge towards the ground truth. The error function used is RMS Euclidean distance. In the graph for the liver contour (Figure 5.6), there is actually an increase in the error from iteration steps 50 to 160. This coincides with the local deformation step and is the result of one of the issues with CT images, which is the non-distinct edges between body parts. The edge between the liver and the wall of the body cavity is very unclear, and often, there is no edge between them. Hence there are no edges for the deformation algorithm to register to. This results in the contour overstepping the boundaries of the liver. Figure 5.8 illustrates this, with the red arrows pointing to the areas where the non-distinct edges between cavity wall and liver causes an error in the deformation. This issue is resolved by having an algorithm determining the inner cavity wall and constraining the liver to never cross this boundary via collision management.
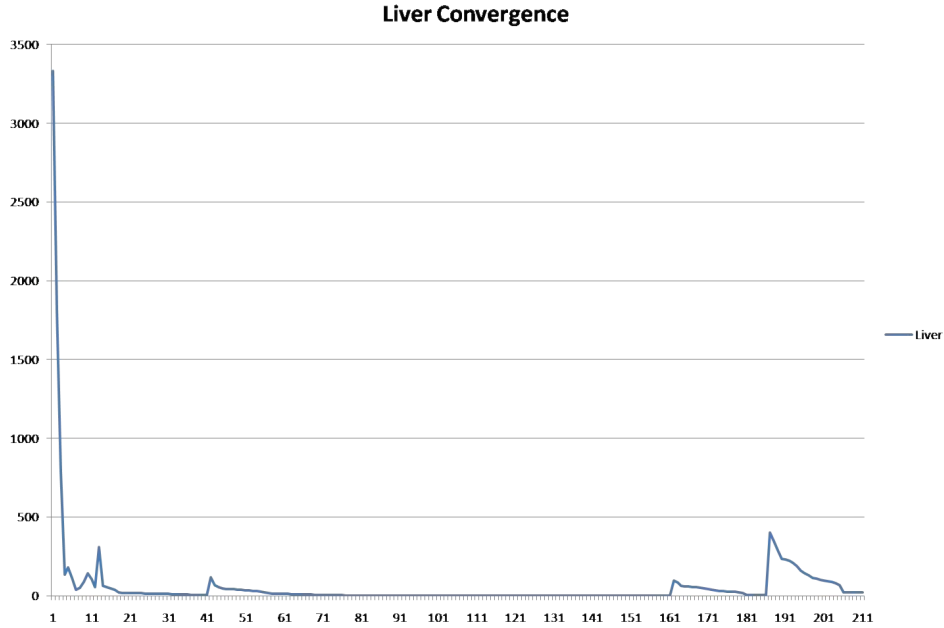
Figure 5.2: Graph for the contour on the liver in one image showing that the contours always converge to a minima at every stage.

5.3 Accuracy

In order to measure the accuracy of the algorithm, the ground truth of a set of CT images was obtained by manually segmenting the various organs from a set of CT images. This work was performed by colleagues working in the faculty. Figure 5.5 is an example of a ground truth contour. By measuring the degree of match between the final registered contour and the edges in the ground truth, the accuracy of the algorithm can be determined. The converged contours are compared to the ground truth using RMS distance to the closest point in the ground truth.

Figures 5.9 and 5.10 show the graphs comparing the registered contours of the liver and stomach respectively to their ground truth contours. This is done for an entire dataset. The values for the liver contours are consistently low, with an mean value of 2.211. The mean value for the stomach is higher at 2.677. This is partly due to the complexity of the stomach as compared to the liver, and also partly due to the diversity in shape of the stomach. This is particularly true in the first few images, in which the stomach does not have a significant air
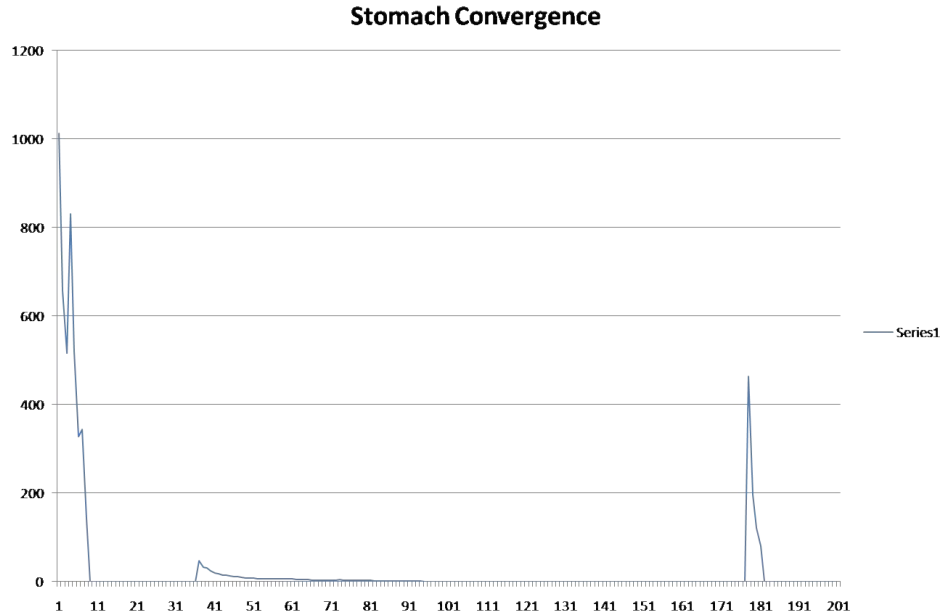
Figure 5.3: Graph for the contour on the stomach in one image showing that the contours always converge to a minima at every stage.

pocket and are of very different shape from the atlas. This results in rather poor accuracy in those images. The accuracy gradually improves as the shape of the stomach slowly changes into something closer to the shape used as an atlas.

5.4 Robustness

In order to test the robustness of the algorithm, datasets from different subjects were obtained and the algorithm was used to find the objects of interest.

The results in Figure 5.11 show that the algorithm is more reliable for extraction of the liver contour than the stomach contour. This is largely due to the liver having a more consistent shape. Therefore, the deviation of the target shape from that in the atlas is generally small. On the other hand, the shape of the stomach varies greatly between each dataset. This is a common problem with soft tissue. The result of this is that it makes it difficult for the algorithm to reliably segment the stomach contour. In this case, a statistical model may
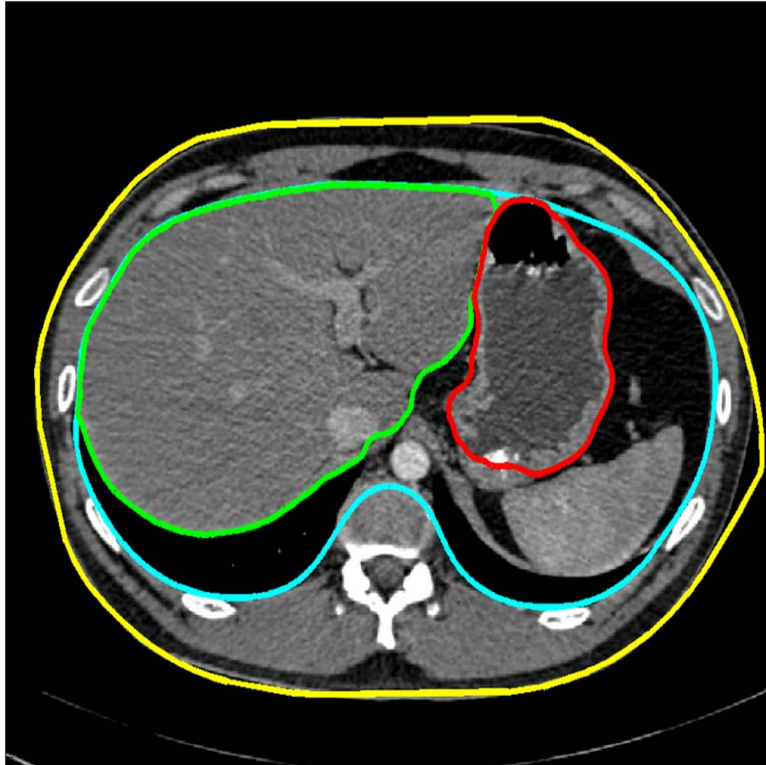
Figure 5.4: Target image used for plotting of graph to test for convergence to ground truth.
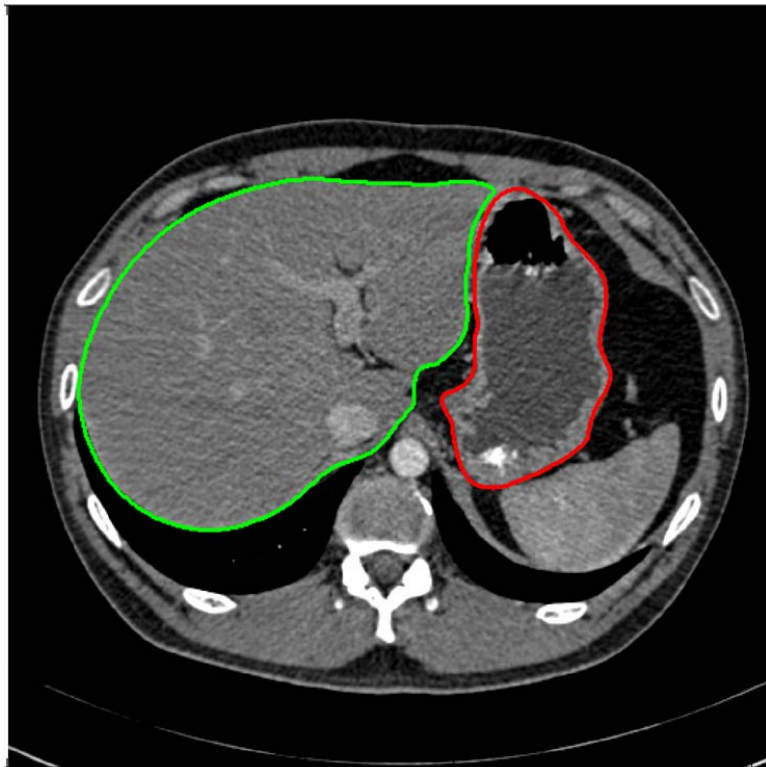
Figure 5.5: Ground truth for the target image in Figure 5.4.
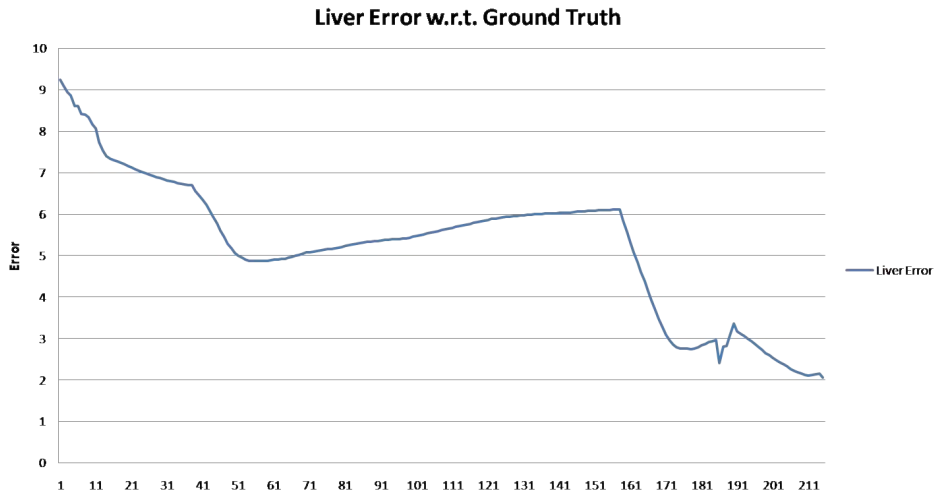
Figure 5.6: Graph for the contour on the liver in one image with the error between the contour and the ground truth plotted against the iteration number.
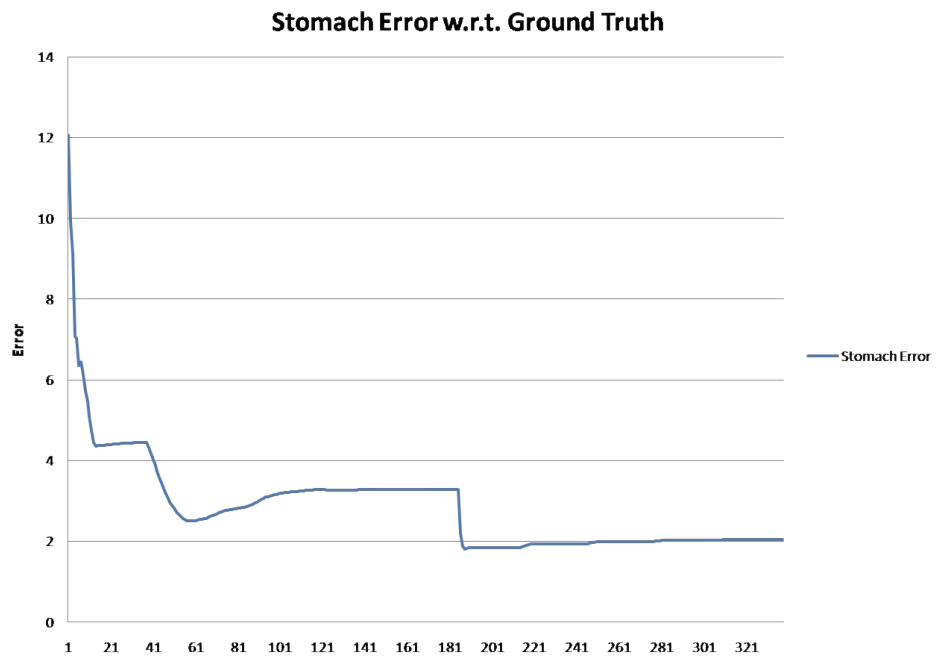
Figure 5.7: Graph for the contour on the stomach in one image with the error between the contour and the ground truth plotted against the iteration number.

64

Figure 5.8: Illustration of the liver contour flowing into the inner body cavity wall due to the non-distinct edges between the wall and the liver.

Figure 5.9: Plot of the degree of match of a registered contour of the liver with the ground truth. The average error is 2.211
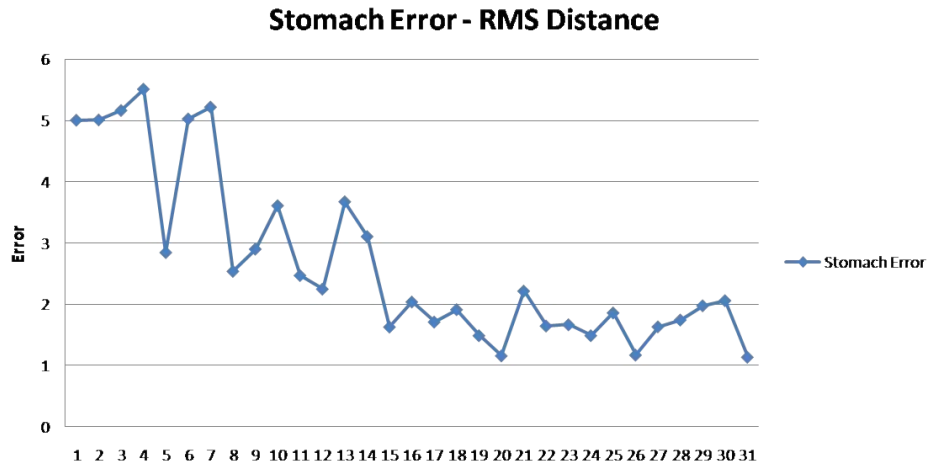
Figure 5.10: Plot of the degree of match of a registered contour of the stomach with the ground truth. The average error is 2.677

be more appropriate, though the challenges in obtaining reliable training data may prohibit such an approach. Nevertheless, the algorithm is s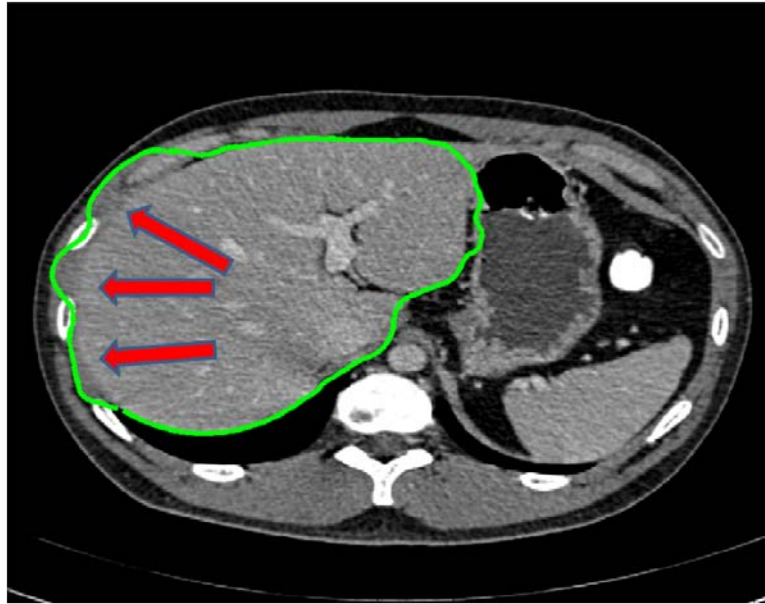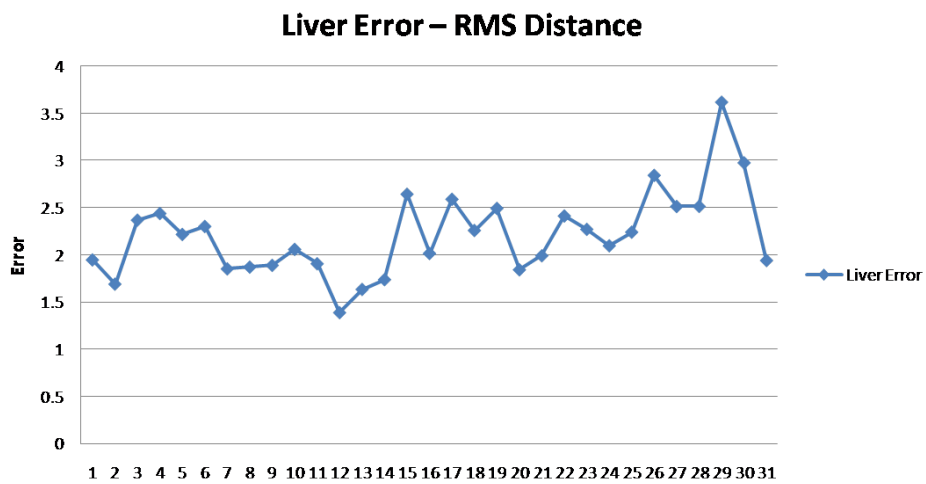till able to successfully register to some stomach contours. This is largely due to the use of intensity gradients in addition to shape and location information. The intensity gradients are largely similar despite the variations in shape, so the registration algorithm is still able to converge the correct region in the CT image, albeit with a reduced accuracy of the contour.

Furthermore, due to the significant variation in the shapes of objects in these new datasets as compared to the atlas, there were cases where the algorithm fails altogether. There are two main reasons for this. The first reason has to do with the use of an atlas with is very different from the dataset, and hence can be easily fixed by using a slice from the dataset as the atlas. The second reason is the robustness of the inner cavity extraction. As the inner cavity wall can be very poorly defined in some cases, the algorithm may fail to segment the inner cavity properly. This in turn falsely constrains the contours for the organs, resulting in a wrong segmentation. Figures 5.12 and 5.13 show some examples of failed segmentations

5.5 Comparison with previous work

The results shown in Ding et al's paper included some images of good fits and some of ill fits. In this comparison, the same CT images were used as the targets for the proposed algorithm. This makes it easier to compare the differences between the two algorithms. The image used as the atlas for Ding et al.'s work and this thesis is the same. The contours segmented from this image were done manually, so while they are largely similar, some differences are bound to be present.

Figures 5.14 to 5.18 show the results of registration using the algorithm proposed in this thesis compared with results produced by Ding et al. From observations of all the comparisons, the proposed algorithm performs at least as well as Ding's algorithm, with several instances of the proposed algorithm out-performing the previous work. This is especially true in the case of the stomach contours, where the proposed algorithm is able to consistently capture the air pocket in the stomach (Figure 5.14).

However, the technique used to locate the air pocket in the stomach has its pitfalls as well. The top left image in Figure 5.15 shows the stomach contour wrongly including some empty space. This issue is mainly due to the appearance of the stomach in the atlas image being significantly different from the target. Removing the technique improves the accuracy of the registration, as shown in figure 5.19. However it would be better to have a different atlas which more closely resembles the stomach in the target image.

5.6 Summary

The tests performed on the algorithm seek to prove its correctness, accuracy and robustness. This was achieved with acceptable results. In comparison with previous work done on the same topic, the proposed algorithm shows a significant improvement in the ability to detect the correct contours as well as the ability to factor in the presence of air pockets in the stomach during segmentation.
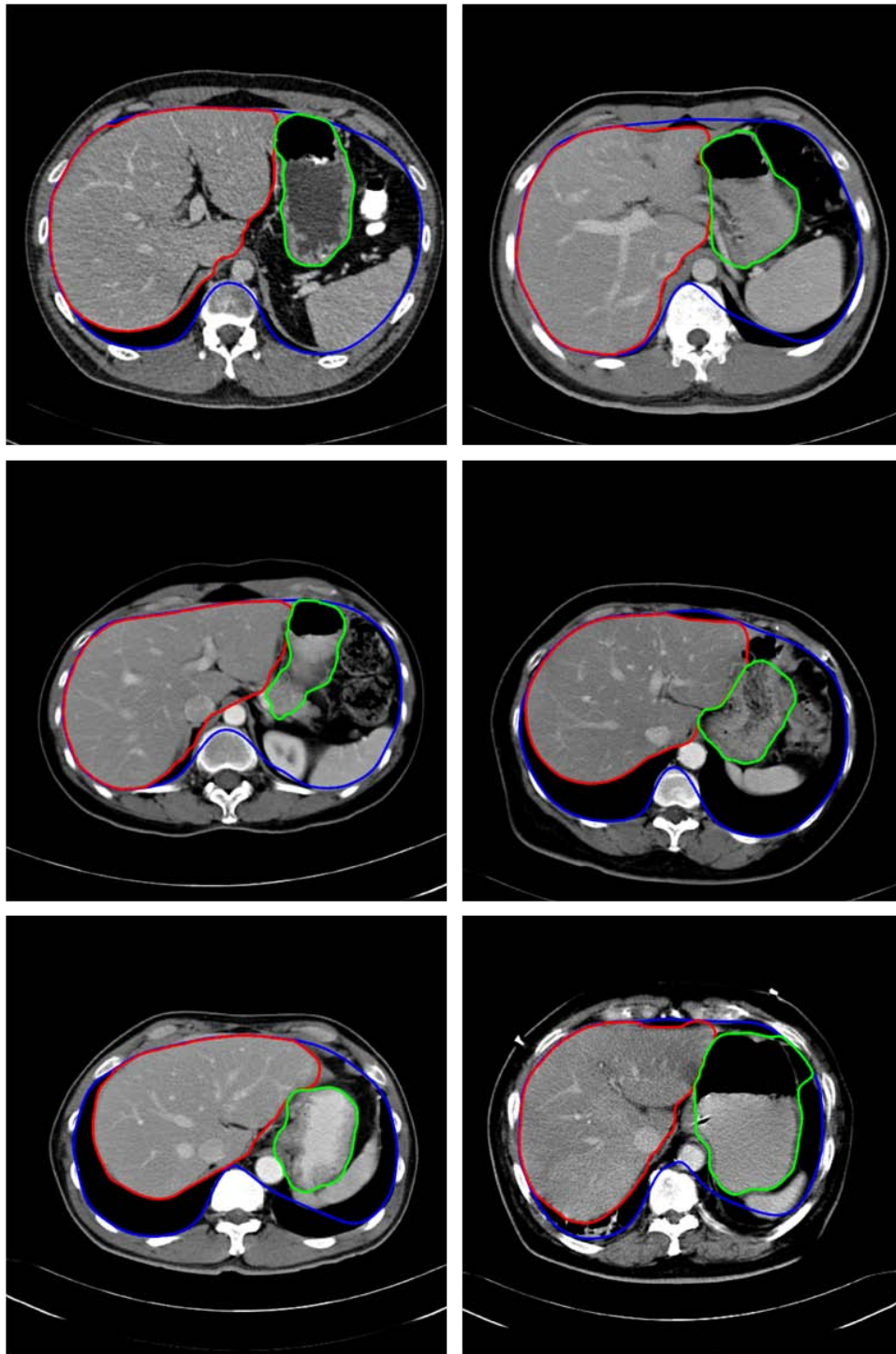
Figure 5.11: Registration results for different data sets
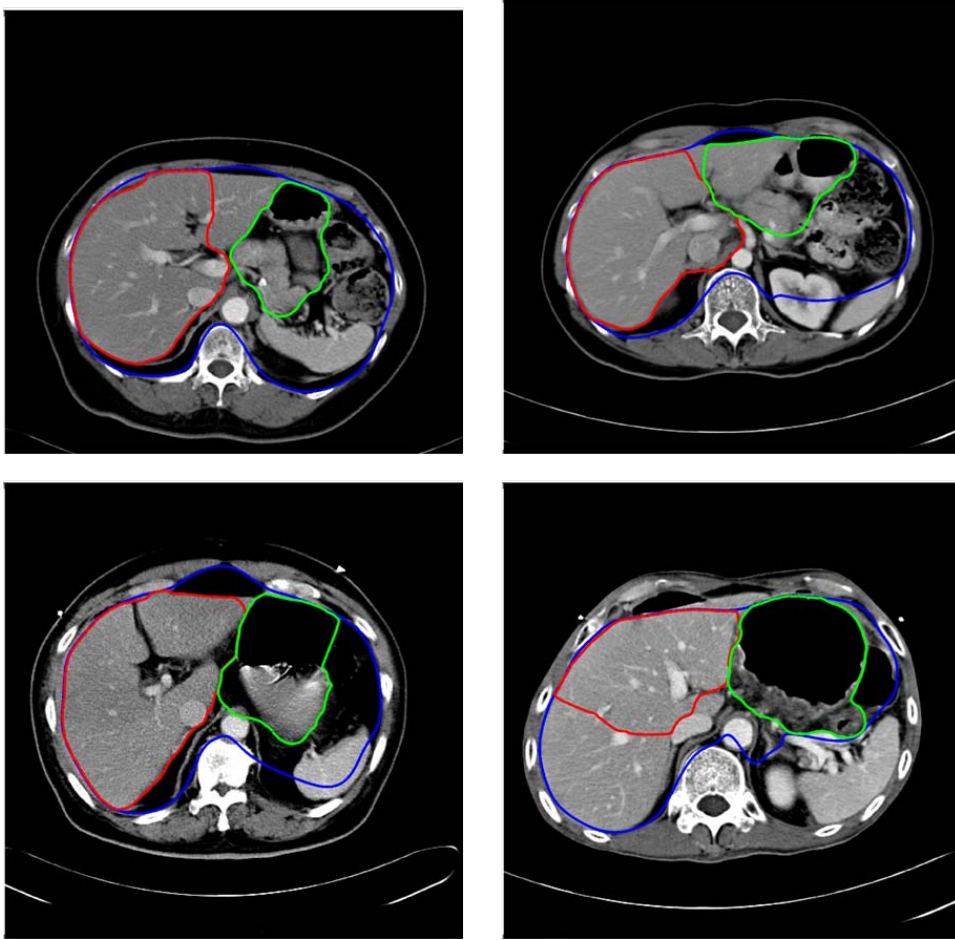
Figure 5.12: Failed registration results due to significant variation from the atlas
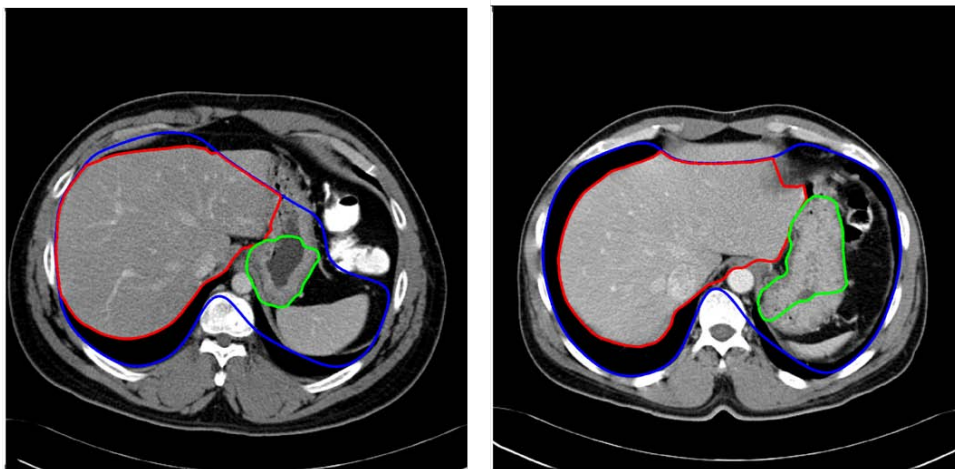
Figure 5.13: Failed registration results due to failed segmentation of inner body cavity
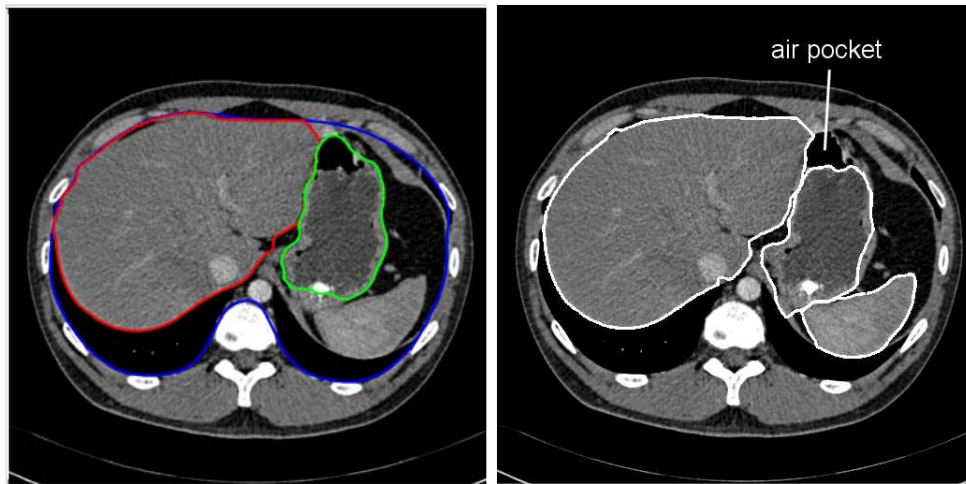
Figure 5.14: The new proposed algorithm(left) can capture the air pockets in the stomach which is not always the case with previous work(right).
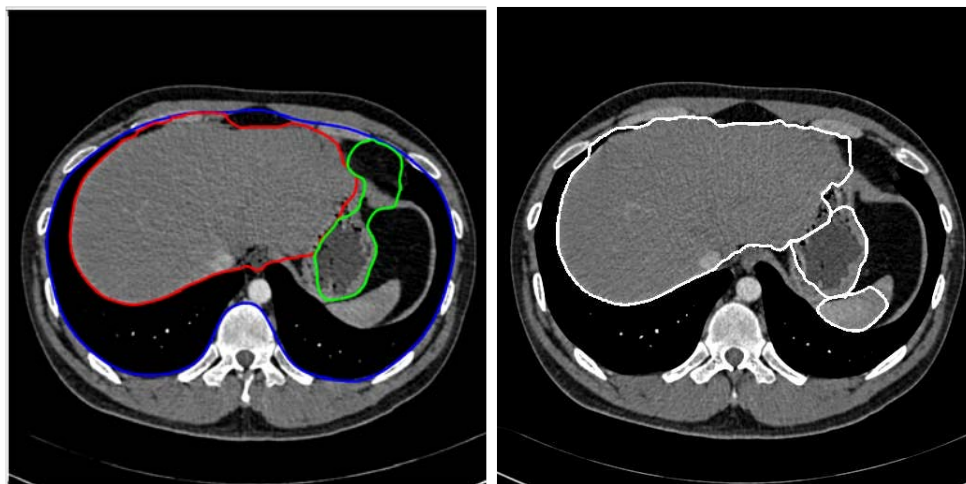
Figure 5.15: Comparison between the proposed algorithm and previous work. Image number is 40
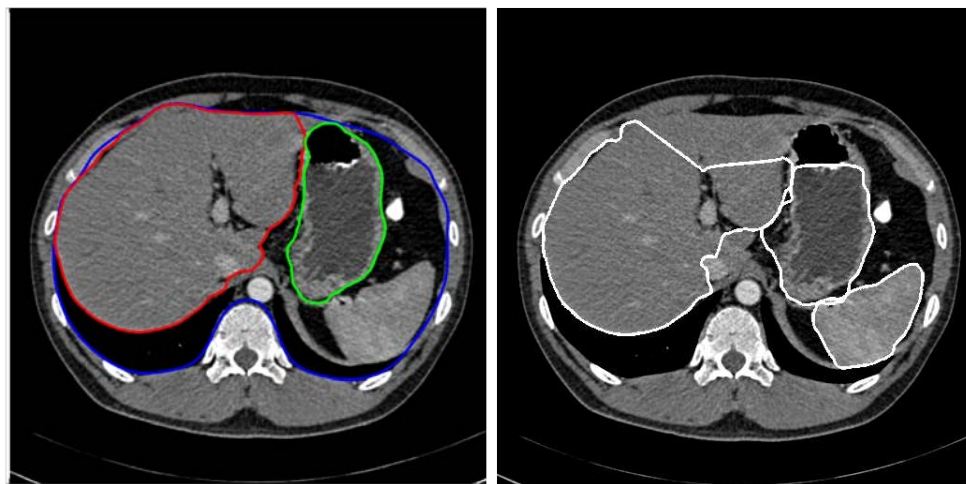
Figure 5.16: Comparison between the proposed algorithm and previous work. Image number is 77
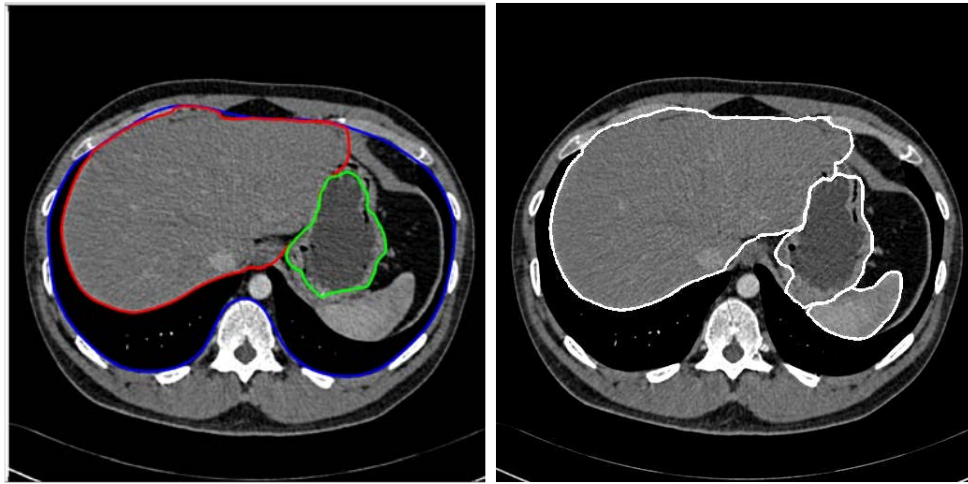
Figure 5.17: Comparison between the proposed algorithm and previous work. Image number is 49
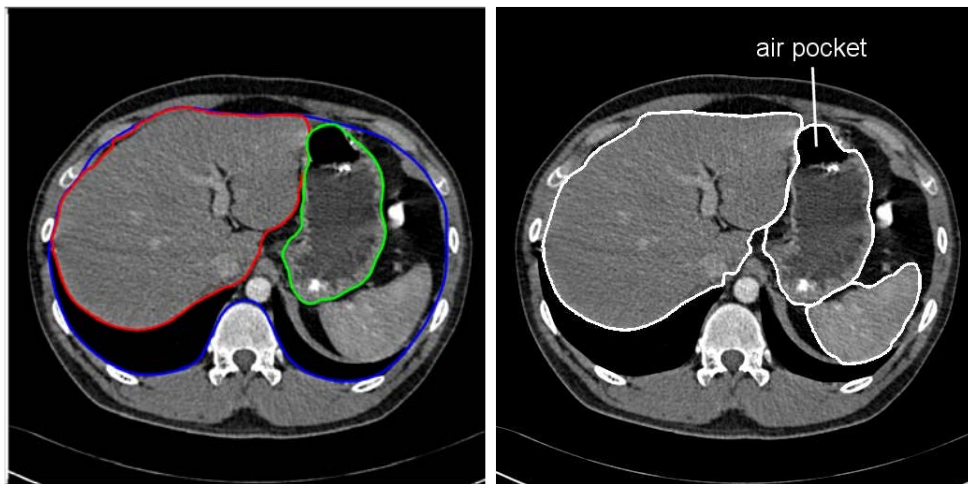
Figure 5.18: Comparison between the proposed algorithm and previous work. Image number is 73
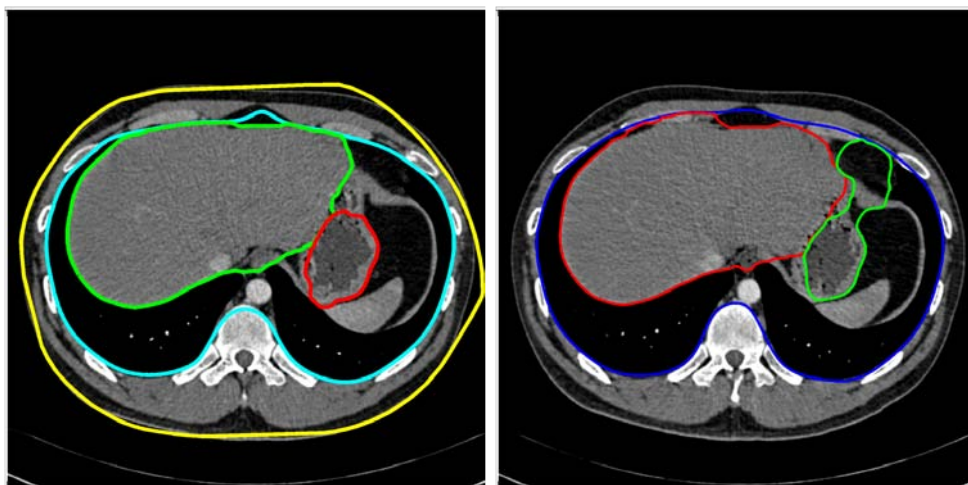
Figure 5.19: Removing the air pocket detection technique improves the result as shown in the image on the right. The image on the left shows the result with air pocket detection

Chapter 6

Conclusion

With the increase in usage of Computer Assisted Surgery in modern day medicine, medical image segmentation is gaining in importance as a tool to assist with treatment. It is extensively used in pre-operational planning, visualization during procedures and even during post-operational monitoring. Therefore, algorithms used in medical image segmentation must be robust, accurate and precise. It should also be as automated as possible to reduce the amount of human error.

This thesis proposes a segmentation framework capable of segmenting different body parts by simply replacing the atlas. The abdominal region of the body is used in this thesis due to availability of data and the challenge posed by the complicated nature of the anatomy. This framework is robust and the results obtained are accurate.

The atlas-based segmentation algorithm proposed uses a non-probabilistic atlas and a multi-stage pipeline approach to automatically register the atlas contours to the target image. The algorithm includes one stage of global registration via ICP and two local deformation stages . The first local deformation stage is the Iterative Corresponding Points algorithm, following by Iterative Corresponding Snakes for the second local deformation stage. Collision detection and resolution are also incorporated into the algorithm to ensure that the various contours in the atlas do not overlap after registration.

The algorithm was shown to be about to accurately segmented the liver and stomach from a set of data. The same atlas was used for 30 slices of CT image with good results.

Also, the atlas was applied to CT images from different datasets. The ability to be able to handle the various variations in shape and location of the organs in the CT images show the robustness of the algorithm. The results obtained were also accurate except for a few cases where the shape variations were too large for the atlas to handle. A change of atlas would be able to resolve these issues.

6.1   Future Work

While the proposed algorithm is able to accurately segment the liver and stomach from CT images, there are still areas which can be improved upon, in order to further enhance the robustness and accuracy of the algorithm.

Firstly, it was observed that the body cavity segmentation fails quite often, especially in cases where the shape variation defers from the atlas by a significant amount. This results in inaccurate matches as the organ contours will be falsely constrained by the body cavity contour. Improving the robustness of the body cavity segmentation will further improve the results achievable by this algorithm.

Secondly, the segmentation done in this proposal is on a slice by slice basis. While the results are reasonable, there is a possibility that the three-dimensional shape will not be correct as there was no inter-slice constraints placed on the algorithm to ensure smooth changes in shape from slice to slice. One future work would be to introduce some inter-slice constraints to the algorithm so that smooth and accurate three-dimensional models of the segmented objects can be produced.

Finally, so far only the abdomen has been used with the algorithm. Other body regions and other image modalities should be tested to determine if the algorithm can be extended to other uses.

Bibliography

[Abe and Matsuzawa, 2000] Abe, T. and Matsuzawa, Y. (2000). Multiple active contour models with application to region extraction. In *ICPR '00: Proceedings of the International Conference on Pattern Recognition*, page 1626, Washington, DC, USA. IEEE Computer Society.

[Al-Zubi et al., 2002] Al-Zubi, S., Toennies, K., Bodammer, N., and Hinrichs, H. (2002). Fusing markov random fields with anatomical knowledge and shape based analysis to segment multiple sclerosis white matter lesions in magnetic resonance images of the brain. In *Bildverarbeitung fur die Medizin*, pages 185–188.

[Arifin and Asano, 2006] Arifin, A. Z. and Asano, A. (2006). Image segmentation by histogram thresholding using hierarchical cluster analysis. *Pattern Recogn. Lett.*, 27(13):1515–1521.

[Atkins and Mackiewich, 1996] Atkins, M. S. and Mackiewich, B. T. (1996). Fully automatic segmentation of the brain in MRI. *IEEE Trans. Medical Imaging*, 17:98–107.

[Baillard et al., 2001] Baillard, C., Hellier, P., and Barillot, C. (2001). Segmentation of brain 3D MR images using level sets and dense registration. *Medical Image Analysis*, 5(3):185–194.

[Ballerini and Bocchi, 2003] Ballerini, L. and Bocchi, L. (2003). Multiple genetic snakes for bone segmentation. In *Applications of evolutionary computing*, pages 346–356.

[Barber et al., 1996] Barber, B. C., Dobkin, D. P., and Huhdanpaa, H. (1996). The quickhull algorithm for convex hulls. *ACM Transactions on Mathematical Software*, 22(4):469–483.

[Besl and Mckay, 1992] Besl, P. J. and Mckay, H. D. (1992). A method for registration of 3-d shapes. *Pattern Analysis and Machine Intelligence, IEEE Transactions on*, 14(2):239–256.

[Bondiau et al., 2005] Bondiau, P.-Y., Malandain, G., Chanalet, S., Marcy, P.-Y., Habrand, J.-L., Fauchon, F., Paquis, P., Courdi, A., Commowick, O., Rutten, I., and Ayache, N. (2005). Atlas-based automatic segmentation of MR images: Validation study on the brainstem in radiotherapy context. *Int. J. of Radiation Oncology Biology Physics*, 61(1):289–298.

[Bosc et al., 2003] Bosc, M., Heitz, F., and Armspach, J.-P. (2003). Statistical atlas-based sub-voxel segmentation of 3D brain MRI. In *ICIP(2)*, pages 1077–1080.

[Boscolo et al., 2002] Boscolo, R., Brown, M. S., and McNitt-Gray, M. F. (2002). Medical image segmentation using knowledge-guided robust active contours. *RadioGraphics*, 22:437–448.

[Brejl and Sonka, 1998] Brejl, M. and Sonka, M. (1998). Edge-based image segmentation: machine learning from examples. *Neural Networks Proceedings, 1998. IEEE World Congress on Computational Intelligence. The 1998 IEEE International Joint Conference on*, 2:814–819 vol.2.

[Chen et al., 2008] Chen, B., Yuen, P.-C., Lai, J.-H., and Chen, W.-S. (2008). A new statistical active contour model for noisy image segmentation. In *CISP '08: Proceedings of the 2008 Congress on Image and Signal Processing, Vol. 3*, pages 226–230, Washington, DC, USA. IEEE Computer Society.

[Chen et al., 2009] Chen, G., Gu, L., Qian, L., and Xu, J. (2009). An improved level set for liver segmentation and perfusion analysis in mris. *IEEE transactions on information technology in biomedicine : a publication of the IEEE Engineering in Medicine and Biology Society*, 13(1):94–103.

[Chen and Liu, 2005] Chen, J. and Liu, S. (2005). A medical image segmentation method based on watershed transform. In *CIT '05: Proceedings of the The Fifth International Conference on Computer and Information Technology*, pages 634–639, Washington, DC, USA. IEEE Computer Society.

[Chen et al., 2005] Chen, Y., Ee, X., Leow, W. K., and Howe, T. S. (2005). T.s.: Automatic extraction of femur contours from hip x-ray images. In *In: Proc. ICCV Workshop on Computer Vision for Biomedical Image Applications*, pages 200–209.

[Chen et al., 2003] Chen, Y., Huang, F., Tagare, H. D., Rao, M., Wilson, D., and Geiser, E. A. (2003). Using prior shape and intensity profile in medical image segmentation. In *Proceedings of Ninth IEEE International Conference on Computer Vision.*

[Chen and Tseng, 2008] Chen, Y. T. and Tseng, D. C. (2008). Medical image segmentation based on the bayesian level set method. pages 25–34.

[Cootes et al., 1994] Cootes, T. F., Hill, A., Taylor, C. J., and Haslam, J. (1994). The use of active shape models for locating structures in medical images. *Image and Vision Computing*, 12(6):355–366.

[Cremers et al., 2007] Cremers, D., Rousson, M., and Deriche, R. (2007). A review of statistical approaches to level set segmentation: Integrating color, texture, motion and shape. *Int. J. Comput. Vision*, 72(2):195–215.

[Cremers et al., 2001] Cremers, D., Schnorr, C., and Weickert, J. (2001). Diffusion-snakes: Combining statistical shape knowledge and image information in a variational framework. In *VLSM '01: Proceedings of the IEEE Workshop on Variational and Level Set Methods (VLSM'01)*, page 137, Washington, DC, USA. IEEE Computer Society.

[Cuadra et al., 2003] Cuadra, B. M., Polio, O., Bardera, A., Cuisenaire, O., Villemure, J.-G., and Thiran, J.-P. (2003). Atlas-based segmentation of pathological brain MR images. In *Proc. Int. Conf. Image Processing*, pages 573–576.

[Cuadra et al., 2004] Cuadra, B. M., Pollo, C., Bardera, A., Cuisenaire, O., Villemure, J.-G., and Thiran, J.-P. (2004). Atlas-based segmentation of pathological MR brain images using a model of lesion growth. *IEEE Trans. Medical Imaging*, 23(10):1301–1314.

[Cuadra et al., 2001] Cuadra, M. B., Cuisenaire, O., Meuli, R., and Thiran, J.-P. (2001). Automatic segmentation of internal structures of the brain in MR images using a tandem of affine and non-rigid registration of an anatomical brain atlas. In *Proc. Int. Conf. Image Processing*, pages 1083–1086.

[Dawant et al., 1999] Dawant, B. M., Hartmann, S. L., Thirion, J.-P., Maes, F., Vandermeulen, D., and Demaerel, P. (1999). Automatic 3-D segmentation of internal structures of head in MR images using a combination of similarity and free-form transformations:

Part I, methodology and validation on normal subjects. *IEEE Trans. Medical Imaging*, 18(10):909–916.

[Ding et al., 2005] Ding, F., Leow, W. K., and Wang, S.-C. (2005). Segmentation of 3D CT volume images using a single 2D atlas. In *Proc. ICCV Workshop on Computer Vision for Biomedical Image Applications (CVBIA 2005), LNCS 3765*, pages 459–468.

[Droske et al., 2001] Droske, M., Meyer, B., Rumpf, M., and Schaller, C. (2001). An adaptive level set method for medical image segmentation. In *IPMI '01: Proceedings of the 17th International Conference on Information Processing in Medical Imaging*, pages 416–422, London, UK. Springer-Verlag.

[Duay et al., 2005] Duay, V., Houhou, N., and Thiran, J. (2005). Atlas-based segmentation of medical images locally constrained by level sets. *Proc. Int. Conf. Image Processing.*

[Elmoataz and Bloyet, 2000] Elmoataz, A. and Bloyet, D. (2000). Image segmentation via multiple active contour models and fuzzy clustering with biomedical applications. In *ICPR '00: Proceedings of the International Conference on Pattern Recognition*, page 1622, Washington, DC, USA. IEEE Computer Society.

[Godbole and Amin, 1995] Godbole, S. and Amin, A. (1995). Mathematical morphology for edge and overlap detection for medical images. *Real-Time Imaging*, 1(3):191–201.

[Grau et al., 2004] Grau, V., Mewes, A. U. J., Alcaniz, M., Kikinis, R., and Warfield, S. K. (2004). Improved watershed transform for medical image segmentation using prior information. *Medical Imaging, IEEE Transactions on*, 23(4):447–458.

[Haris et al., 1998] Haris, K., Estradiadis, S. N., Maglaveras, N., and Katsaggelos, A. K. (1998). Hybrid image segmentation using watersheds and fast region merging. *IEEE Transactions on Image Processing*, 7(12):1684–1699.

[Hartmann et al., 1999] Hartmann, S. L., Parks, M. H., Martin, P. R., and Dawant, B. M. (1999). Automatic 3-D segmentation of internal structures of head in MR images using a combination of similarity and free-form transformations: Part II, validation on severely atrophied brains. *IEEE Trans. Medical Imaging*, 18(10):917–926.

[Kass et al., 1987] Kass, M., Witkin, A., and Terzopoulos, D. (1987). Snakes: Active contour models. *Int. J. Computer Vision*, 1(4):321–331.

[Keleman et al., 1998] Keleman, A., Szekely, G., and Gerig, G. (1998). Three-dimensional model-based segmentation of brain MRI. *IEEE Workshop on Biomedical Image Analysis*, 00.

[Kim and Hong, 2008] Kim, J.-S. and Hong, K.-S. (2008). A new graph cut-based multiple active contour algorithm without initial contours and seed points. *Mach. Vision Appl.*, 19(3):181–193.

[Lee et al., 2007] Lee, J., Kim, N., Lee, H., Seo, J. B., Won, H. J., Shin, Y. M., Shin, Y. G., and Kim, S.-H. (2007). Efficient liver segmentation using a level-set method with optimal detection of the initial liver boundary from level-set speed images. *Computer Methods and Programs in Biomedicine*, 88(1):26–38.

[Liu et al., 2007a] Liu, C., Ma, J., and Ye, G. (2007a). Medical image segmentation by geodesic active contour incorporating region statistical information. In *FSKD '07: Proceedings of the Fourth International Conference on Fuzzy Systems and Knowledge Discovery (FSKD 2007) Vol.3*, pages 63–67, Washington, DC, USA. IEEE Computer Society.

[Liu et al., 2005] Liu, F., Zhao, B., Kijewski, P. K., Wang, L., and Schwartz, L. H. (2005). Liver segmentation for ct images using gvf snake. *Med Phys*, 32(12):3699–3706.

[Liu and Sclaroff, 2004] Liu, L. and Sclaroff, S. (2004). Deformable model-guided region split and merge of image regions. *Image Vision Comput.*, 22(4):343–354.

[Liu et al., 2007b] Liu, T., Luo, X., Peng, C., and Wen, L. (2007b). Improved morphological edge detection algorithm for ultrasound heart ventricular wall image in the motion of its rotation. pages 960–963.

[Lötjönen et al., 2004] Lötjönen, J., Kivistö, S., Koikkalainen, J., Smutek, D., and Lauerma, K. (2004). Statistical shape model of atria, ventricles and epicardium from short- and long-axis MR images. *Medical Image Analysis*, 8:371–386.

[Mancas et al., 2005] Mancas, M., Gosselin, B., and Macq, B. (2005). Segmentation using a region-growing thresholding. volume 5672, pages 388–398. SPIE.

[Martin et al., 2004] Martin, R., Bordes, N., Hugh, T., and Pailthorpe, B. (2004). Semi-automatic feature delineation in medical images. In *APVis '04: Proceedings of the 2004 Australasian symposium on Information Visualisation*, pages 127–131, Darlinghurst, Australia, Australia. Australian Computer Society, Inc.

[Massoptier and Casciaro, 2007] Massoptier, L. and Casciaro, S. (2007). Fully Automatic Liver Segmentation through Graph-Cut Technique. In *29th Annual International Conference of the IEEE Engineering in Medicine and Biology Society*, pages 5243–5246.

[Mille et al., 2007] Mille, J., Bone, R., Makris, P., and Cardot, H. (2007). Segmentation and tracking of the left ventricle in 3d mri sequences using an active surface model. In *CBMS '07: Proceedings of the Twentieth IEEE International Symposium on Computer-Based Medical Systems*, pages 257–262, Washington, DC, USA. IEEE Computer Society.

[Mitchell et al., 2001] Mitchell, S. C., Lelieveldt, B. P. F., Geest, R. J. V. D., Bosch, H. G., Reiber, J. H. C., and Sonka, M. (2001). Multistage hybrid active appearance model matching: Segmentation of left and right ventricles in cardiac MR images. *IEEE Trans. Medical Imaging*, 20:415–423.

[Okada et al., 2007] Okada, T., Shimada, R., Sato, Y., Hori, M., Yokota, K., Nakamoto, M., Chen, Y. W., Nakamura, H., and Tamura, S. (2007). Automated segmentation of the liver from 3d ct images using probabilistic atlas and multi-level statistical shape model. *Medical image computing and computer-assisted intervention : MICCAI ... International Conference on Medical Image Computing and Computer-Assisted Intervention*, 10(Pt 1):86–93.

[Park et al., 2003] Park, H., Bland, P. H., and Meyer, C. R. (2003). Construction of an abdominal probabilistic atlas and its application in segmentation. *IEEE Trans. Medical Imaging*, 22(4):483–492.

[Pohle and Toennies, 2001] Pohle, R. and Toennies, K. D. (2001). A new approach for model-based adaptive region growing in medical image analysis. *Lecture Notes in Computer Science*, 2124:238–??

[Prastawa et al., 2003] Prastawa, M., Bullitt, E., Moon, N., and Leemput, K. V. (2003). Automatic brain tumur segmentation by subject specific modification of atlas priors. *Academic Radiology*, 10:1341–1348.

[Prastawa et al., 2005] Prastawa, M., Gilmore, J. H., Lin, W., and Gerig, G. (2005). Automatic segmentation of MR images of the developing newborn brain. *Medical Image Analysis*.

[Rigau et al., 2004] Rigau, J., Feixas, M., Sbert, M., Bardera, A., and Boada, I. (2004). Medical image segmentation based on mutual information maximization. In *In International Conference on Medical Image Computing and Computed Assisted Intervention (MICCAI 2004), Proceedings, Rennes-Saint*, pages 135–142. Springer.

[Sandor and Leahy, 1997] Sandor, S. and Leahy, R. (1997). Surface-based labeling of cortical anatomy using a deformable atlas. *IEEE Transactions on Medical Imaging*, 16(1):41–54.

[Shen and Davatzikos, 2000] Shen, D. and Davatzikos, C. (2000). An adaptive-focus deformable model using statistical and geometric information. *IEEE Trans. Pattern Analysis and Machine Intelligence*, 22(8):906–913.

[Shen et al., 2001] Shen, D., Herskovits, E. H., and Davatzikos, C. (2001). An adaptive-focus statistical shape model for segmentation and shape modeling of 3-D brain structures. *IEEE Trans. Medical Imaging*, 20(4):257–270.

[Shen et al., 2004] Shen, D., Lao, Z., Zeng, J., Zhang, W., Sesterhenn, I. A., Sun, L., Moul, J. W., Herskovits, E. H., Fichtinger, G., and Davatzikos, C. (2004). Optimized prostate biopsy via a statistical atlas of cancer spatial distribution. *Medical Image Analysis*, 8(2):139–150.

[Silveira and Marques, 2006] Silveira, M. and Marques, J. (2006). Automatic segmentation of the lungs using multiple active contours and outlier model. In *Engineering in Medicine and Biology Society, 2006. EMBS '06. 28th Annual International Conference of the IEEE*, pages 3122–3125, Washington, DC, USA. IEEE Computer Society.

[Slabaugh et al., 2006] Slabaugh, G., Unal, G., Fang, T., and Wels, M. (2006). Ultrasound-specific segmentation via decorrelation and statistical region-based active contours. In *CVPR '06: Proceedings of the 2006 IEEE Computer Society Conference on Computer Vision and Pattern Recognition*, pages 45–53, Washington, DC, USA. IEEE Computer Society.

[Sluimer et al., 2005] Sluimer, I., Prokop, M., and van Ginneken, B. (2005). toward automated segmentation of the pathological lung in CT. *IEEE Transactions on Medical Imaging*, 24(8):1025–1038.

[Straka et al., 2003a] Straka, M., Cruz, A. L., Kchl, A., rmek, M., Fleischmann, D., and Grller, E. (2003a). 3d watershed transform combined with a probabilistic atlas for medical image segmentation. In *Proceedings of MIT 2003*, pages 1–8.

[Straka et al., 2003b] Straka, M., LaCruz, A., Dimitrov, L. I., Srámek, M., Fleischmann, D., and Groller, E. (2003b). Bone segmentation in CT-angiography data using a probabilistic atlas. In *Proc. Conf. on Vision Modeling and Visualization*, pages 505–512.

[Tobias and Seara, 2002] Tobias, O. J. and Seara, R. (2002). Image segmentation by histogram thresholding using fuzzy sets. *IEEE Transactions on Image Processing*, 11(12):1457–1465.

[Vemuri et al., 2003] Vemuri, B. C., Ye, J., Chen, Y., and Leonard, C. M. (2003). Image registration via level-set motion: Applications to atlas-based segmentation. *Medical Image Analysis*, 7(1):1–20.

[Wang and Staib, 2000] Wang, Y. and Staib, L. H. (2000). Physical model-based non-rigid registration incorporating statistical shape information. *Medical Image Analysis*, 4(1):7–20.

[Xu and Prince, 1998] Xu, C. and Prince, J. L. (1998). Snakes, shapes, and gradient vector flow. *IEEE Transactions on Image Processing*, 7(3):359–369.

[Xue et al., 2001] Xue, J. H., Ruan, S., Moretti, B., Revenu, M., and Bloyet, D. (2001). Knowledge-based segmentation and labeling of brain structures from MRI images. *Pattern Recognition Letters*, 22:395–405.

[Yang et al., 2008] Yang, Y., Huang, S., Lin, P., and Rao, N. (2008). Medical image segmentation based on level set combining with region information. In *ICNC '08: Proceedings of the 2008 Fourth International Conference on Natural Computation*, pages 70–74, Washington, DC, USA. IEEE Computer Society.

[Yezzi and Tannenbaum, 2002] Yezzi, A. J. and Tannenbaum, A. (2002). 4d active surfaces for cardiac analysis. In *MICCAI '02: Proceedings of the 5th International Conference on Medical Image Computing and Computer-Assisted Intervention-Part I*, pages 667–673, London, UK. Springer-Verlag.

[Yushkevich et al., 2006] Yushkevich, P. A., Piven, J., Hazlett, H. C., Smith, R. G., Ho, S., Gee, J. C., and Gerig, G. (2006). User-guided 3d active contour segmentation of anatomical structures: significantly improved efficiency and reliability. *Neuroimage*, 31(3):1116–1128.

[Zhang and Braun, 1997] Zhang, Z. and Braun, M. (1997). Fully 3d active surface models with self–inflation and self–deflation forces. In *CVPR '97: Proceedings of the 1997 Conference on Computer Vision and Pattern Recognition (CVPR '97)*, page 85, Washington, DC, USA. IEEE Computer Society.